Taylor & Francis
Taylor & Francis Group

Structure and Infrastructure Engineering

Maintenance, Management, Life-Cycle Design and Performance

ISSN: 1573-2479 (Print) 1744-8980 (Online) Journal homepage: http://www.tandfonline.com/loi/nsie20

Numerical prediction of solitary wave forces on a typical coastal bridge deck with girders

Guoji Xu, Chunsheng Cai & Lu Deng

To cite this article: Guoji Xu, Chunsheng Cai & Lu Deng (2016): Numerical prediction of solitary wave forces on a typical coastal bridge deck with girders, Structure and Infrastructure Engineering, DOI: 10.1080/15732479.2016.1158195

To link to this article: http://dx.doi.org/10.1080/15732479.2016.1158195

Published online: 23 Mar 2016.

http://dx.doi.org/10.1080/15732479.2016.1158195

Taylor & Francis
Taylor & Francis Group

Numerical prediction of solitary wave forces on a typical coastal bridge deck with girders

Guoji Xu[a], Chunsheng Cai[b] and Lu Deng[c]

[a]Center for Computation and Technology, Louisiana State University, Baton Rouge, LA, USA; [b]Department of Civil and Environmental Engineering, Louisiana State University, Baton Rouge, LA, USA; [c]College of Civil Engineering, Hunan University, Changsha, China

ABSTRACT

In this study, a numerical method for predicting solitary wave forces on a typical coastal bridge deck with girders is utilised in order to obtain an alternative way to assess solitary wave forces on coastal bridge decks with sufficient accuracy. Firstly, a wave model based on the solitary wave theory representing the incident wave of tsunamis is applied through a computational fluid dynamics computer program, where the shear stress transport *k*-*ω* model is adopted as the turbulent closure for the Reynolds Averaged Navier–Stokes model equations. Then, the numerical wave profiles and the predicted wave forces are compared with the analytical solutions and the reported laboratory measurements, respectively. These verifications assure the results in the following parametric study reliable. Finally, comparisons between the numerical results and those acquired through the empirical methods are conducted in order to examine the appropriateness of these empirical procedures regarding this specific case. Furthermore, an expanded formula is proposed with the definitions of the key parameters being discussed thereafter. This method can be expanded to cases where different deck cross sections rather than the typical one used in the present study are considered and to scenarios where different wave parameters are involved. It is hoped that the expanded formula could provide straightforward but advisable results for practicing engineers.

ARTICLE HISTORY
Received 17 September 2015
Revised 13 January 2016
Accepted 22 January 2016

KEYWORDS
Wave forces; coastal bridges; submersion depth; wave height; solitary waves

Introduction

Wave forces are responsible for many coastal bridge failures during recent tsunamis (FHWA, 2008; Maruyama et al., 2013; Shoji & Moriyama, 2007; Sugimoto & Unjoh, 2006), and many efforts have been made in order to understand the bridge failures and tsunami wave forces on the bridges. However, due to the complex geometries of coastal bridge superstructures and other variable parameters, such as the bridge site bathymetry, the clearance between the bottom of the superstructure and the still water level (SWL) and the tsunami wave stages (breaking or non-breaking), it is difficult to analyse tsunami wave forces (vertically and horizontally) on bridges using available design approaches such as the current AASHTO procedure (AASHTO, 2008; Douglass & Krolak, 2008) that are primarily proposed for hurricane-induced waves. As such, it is of significant importance to develop alternative tsunami wave-related methodologies in order to appropriately assess the wave loadings on bridge decks for designing or retrofitting coastal bridges in tsunami prone areas.

Some early studies on tsunami waves (French, 1969, 1979; Iradjpanah, 1983; Lai, 1986; Lai & Lee, 1989) mainly focused on the solitary wave (the incident wave of tsunamis)-induced forces on horizontal platforms and elevated slabs. These studies employed conventional laboratory approaches and emerging numerical methods to realise the designated objectives and provide useful observations which have shed some lights on the understandings of the solitary wave forces on bridge superstructures. Recently, the devastating damage of bridges due to the tsunamis has motivated more research using both experimental and numerical methods on the bridge deck-wave interaction problems since the last decade (Azadbakht & Yim, 2014, 2015; Bozorgnia, Lee, & Raichlen, 2010; Hayatdavoodi, Seiffert, & Ertekin, 2014; Lau, Ohmachi, Inoue, & Lukkunaprasit, 2011; McPherson, 2008; Seiffert, Ertekin, & Robertson, 2015; Seiffert, Hayatdavoodi, & Ertekin, 2014). McPherson (2008) conducted a laboratory study with a 1:20 scale bridge model and this bridge model will be utilised later for the verification purpose in the current study. Bozorgnia et al. (2010) carried out numerical simulations for solitary waves on the bridge decks with and without air venting holes. Comparisons of the obtained wave forces between these two cases show the advantages of adopting air venting holes in practice engineering. Seiffert et al. (2014, 2015) and Hayatdavoodi et al. (2014) presented experimental studies for solitary wave forces on a two-dimensional (2D) model of coastal bridge decks with a 1:35 scale. Numerical simulations were calculated using Euler's inviscid model in OpenFOAM in

CONTACT Guoji Xu gxu2@lsu.edu

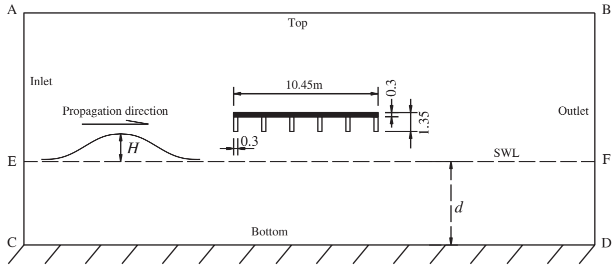

Figure 1. Schematic diagram for the computational domain.

order to make comparisons with the results from the laboratory measurements.

While the above-discussed studies focus on solitary waves only, Lau et al. (2011) and Azadbakht and Yim (2014, 2015) documented the characteristics of tsunami bore forces on the bridge decks and empirical equations with respect to their studied cases were proposed. However, there are quite limited studies touching the topic of proposing design equations for the tsunami incident waves (McPherson, 2008). The physical mechanics between the tsunami bores impinging the bridge deck and tsunami incident waves interacting with the bridge deck can be significant. As such, this study is motivated by proposing an empirical equation for estimating solitary wave forces on typical coastal bridge decks.

In this paper, a numerical method for predicting solitary wave forces on a typical coastal bridge deck with girders is utilised. To this end, a wave model based on the solitary wave theory representing the incident wave of tsunamis is applied at first using a computational fluid dynamics computer program ANSYS Fluent (Academic Version, V15.0), where the shear stress transport (SST) k-ω model is adopted as the turbulent closure for the Reynolds Averaged Navier–Stokes model (RANS) equations. Verification of the wave profiles with analytical solutions and of the wave forces with reported laboratory experiments is then conducted, demonstrating that the utilised numerical method can yield reliable results with sufficient accuracy in the following parametric study. Finally, comparisons between the numerical results and those acquired through the empirical methods are conducted in order to examine the appropriateness of these empirical procedures regarding this specific case. In addition, an expanded formula is proposed with the definitions of the key parameters being discussed thereafter. Further verifications of the expanded method is conducted, which shows a potential and promising application of the proposed expanded method.

Numerical methodology and verification

Governing equations

In the present study, 2D numerical simulations are adopted since significant computational cost can be saved as compared with three dimensional (3D) simulations and reasonable results can be yielded by using 2D simulations on this specific topic pertaining to the bridge deck-wave interaction problems (Bozorgnia & Lee, 2012). For the turbulent flow simulations, water is assumed as an incompressible, viscous fluid. The fluid motion is described based on the Navier–Stokes equations, which are shown as follows:

$$\frac{\partial(\rho u)}{\partial x} + \frac{\partial(\rho v)}{\partial y} = 0 \tag{1a}$$

$$\frac{\partial(\rho u)}{\partial t} + u\frac{\partial(\rho u)}{\partial x} + v\frac{\partial(\rho u)}{\partial y} = -\frac{\partial p}{\partial x} + \mu\left(\frac{\partial^2 u}{\partial x^2} + \frac{\partial^2 u}{\partial y^2}\right) + S_x \tag{1b}$$

$$\frac{\partial(\rho v)}{\partial t} + u\frac{\partial(\rho v)}{\partial x} + v\frac{\partial(\rho v)}{\partial y} = -\frac{\partial p}{\partial y} - \rho g + \mu\left(\frac{\partial^2 v}{\partial x^2} + \frac{\partial^2 v}{\partial y^2}\right) + S_y \tag{1c}$$

where ρ is the mass density, u and v are the velocity components, p is the pressure, μ is the viscosity, g is the gravitational acceleration and S_x and S_y are the momentum sources in the x direction and y direction, respectively.

To account for the turbulent fluctuations in the bridge deck-wave interaction problem, the SST k-ω model is used as the turbulence closure for the RANS equations. This turbulent model has its advantages over the k-ε model, one of the most common turbulence models, such that the flow domain with a high Reynold number and the near wall domain with a relatively low Reynold number can be more appropriately resolved. The equations for this turbulent model are:

$$\frac{\partial}{\partial t}(\rho k) + \frac{\partial}{\partial x_i}\left(\rho k u_i\right) = \frac{\partial}{\partial x_j}\left(\Gamma_k \frac{\partial k}{\partial x_j}\right) + G_k - Y_k + S_k \tag{2a}$$

$$\frac{\partial}{\partial t}(\rho \omega) + \frac{\partial}{\partial x_j}\left(\rho \omega u_j\right) = \frac{\partial}{\partial x_j}\left(\Gamma_\omega \frac{\partial \omega}{\partial x_j}\right) + G_\omega - Y_\omega + D_\omega + S_\omega \tag{2b}$$

where $\Gamma_k = \mu + \frac{\mu_t}{\sigma_k}$ and $\Gamma_\omega = \mu + \frac{\mu_t}{\sigma_\omega}$ are the effective diffusivity of k and ω; σ_k and σ_ω are the turbulent Prandtl numbers for k and ω, respectively; μ_t is the turbulent viscosity; G_k represents the production of turbulence kinetic energy, $G_k = -\rho\overline{u_i' u_j'}\frac{\partial u_j}{\partial x_i}$; $-\rho\overline{u_i' u_j'}$ is Reynolds stress, representing the turbulent flow effects on the mean flow field, $-\rho\overline{u_i' u_j'} = \mu_t\left(\frac{\partial u_i}{\partial x_j} + \frac{\partial u_j}{\partial x_i}\right) - \frac{2}{3}\rho k \delta_{ij}$; k is the turbulent kinetic energy, $k = \frac{1}{2}\overline{u_i' u_i'}$; u_i and u_i' are the mean and fluctuating velocity components; δ_{ij} is Kronecker delta; G_ω is the generation of ω; Y_k and Y_ω are the dissipation of k and ω, respectively; D_ω is the cross-diffusion term; and S_k and S_ω are user-defined source terms. The detailed description of this model can be found in Mentor (1994).

For the set-ups of the SST k-ω model in Fluent, the pressure-based solver (segregated) is chosen for the transient flow, the Pressure-Implicit with Splitting of Operators scheme (Bricker, Kawashima, & Nakayama, 2012; Bricker & Nakayama, 2014; FHWA, 2009) is utilised for the pressure–velocity coupling method, and the PRESTO (PREssure STaggering Option) scheme is set for the pressure spatial discretisation. The turbulence damping is turned on and the damping factor is 50. For the velocity inlet boundary, the turbulent intensity is 2% and turbulent viscosity ratio is 10%. For the top and outlet of the calculation domain (see Figure 1), the backflow turbulent intensity and the backflow turbulent viscosity ratio are the same as that set for the velocity inlet boundary. As a two-phase problem, the volume of fluid (VOF) method (Hirt & Nichols, 1981) is employed to prescribe the dynamic free surface. Least squares cell-based scheme is used for the gradient discretisation, second-order upwind for momentum advection terms and geo-reconstruct for the volume fraction equations. Second-order upwind is also used for the spatial discretisation of the turbulent kinetic energy and the specific dissipation rate.

Theory of the second-order solitary wave

The water particle velocities u and v, water pressure p and free surface profile η of the solitary wave of the second-order (Sarpkaya & Isaacson, 1981) are expressed as follows:

$$\frac{\eta}{d} = \varepsilon \mathrm{sech}^2 q - \frac{3}{4}\varepsilon^2 \mathrm{sech}^2 q \tanh^2 q \tag{3a}$$

$$\frac{p}{\rho g d} = \frac{\eta}{d} + 1 - \frac{s}{d} - \frac{3}{4}\varepsilon^2 \mathrm{sech}^2 q \left[\left(\frac{s}{d}\right)^2 - 1\right]\left(2 - 3\mathrm{sech}^2 q\right) \tag{3b}$$

$$\frac{u}{\sqrt{gd}} = \varepsilon \mathrm{sech}^2 q + \varepsilon^2 \mathrm{sech}^2 q \left\{\frac{1}{4} - \mathrm{sech}^2 q - \frac{3}{4}\left(\frac{s}{d}\right)^2 \left(2 - 3\mathrm{sech}^2 q\right)\right\} \tag{3c}$$

$$\frac{v}{\sqrt{gd}} = \varepsilon \sqrt{3\varepsilon}\left(\frac{s}{d}\right) \mathrm{sech}^2 q \tanh q \left\{1 - \varepsilon\left[\frac{3}{8} + 2\mathrm{sech}^2 q + \frac{1}{2}\left(\frac{s}{d}\right)^2 \left(1 - 3\mathrm{sech}^2 q\right)\right]\right\} \tag{3d}$$

where $\varepsilon = \frac{H}{d}$, $q = \frac{\sqrt{3\varepsilon}}{2d}\left(1 - \frac{5}{8}\varepsilon\right)(x - ct)$, $s = y + d$, d is the still water depth, H is the wave height and y is the distance from the SWL and is negative if it is in the same direction with the gravitational acceleration. Hence, the wave celerity c can be calculated as:

$$\frac{c}{\sqrt{gd}} = 1 + \frac{1}{2}\varepsilon - \frac{3}{20}\varepsilon^2 \tag{4}$$

It is calculated from Equation (3a) that the solitary wave crest is located at $x = 0$ when $t = 0s$, namely, the wave crest is just at the inlet boundary. To more appropriately simulate the wave profile, the incident solitary wave should be shifted leftward by replacing t with $t - t_0$, where $t_0 = L_{\min}/c$ and $L_{\min}$ is defined as the minimum length to allow the wave crest to reach the inlet boundary after a certain time. In this way, the water surface will increase gradually at the inlet boundary to ensure that a fully developed wave profile will be generated propagating from the inlet to the location of the structure model. $L_{\min}$ should be greater than the effective wave length L_e, where $L_e = 2\pi d/\sqrt{\frac{3H}{d}}$. This method was adopted from Dong and Zhan (2009).

Numerical calculation domain and boundary conditions

Figure 1 shows the schematic diagram for the 2D computational domain, where the line EF is the SWL, which separates the regions of the air phase and water phase at the initial point. The geometry of a typical coastal bridge deck model that with six girders is introduced here firstly for the convenience of discussion, and the numerical simulations employing this bridge model will be described later. This prototype bridge designed to carry two traffic lanes on the deck consists of a slab and six AASHTO type III girders and can be commonly found connecting island communities (Hayatdavoodi et al., 2014). The width of the superstructure is 10.45 m, the girder height is 1.05 m and the deck depth is .3 m. All the six girders, each with a width of .3 m, are simplified as rectangles. The railing effect will be considered later for selected cases to demonstrate the effects of the railing height on the wave forces.

The boundary conditions are the same for all the simulations in the present study and are specified as follows:

AB: pressure outlet. This keeps the pressure in the air phase being the static gauge pressure that is the same as the operating pressure (101,325 Pa).

AC: velocity inlet. The equations of u (3c) and v (3d) are compiled into Fluent as the velocity inlet components in the x and y directions, respectively, by the user defined functions. The free surface profile η is controlled by Equation (3a).

CD: No slip stationary wall condition.

BD: pressure outlet.

Verification of the wave profiles with analytical results

To ensure sufficient accuracy for the numerical methodology, a verification of the wave profile with analytical results is deemed as a primary and essential step. In this verification procedure, the computation domain is set with a section of 200 m long and 13 m high. The mesh sensitivity study is conducted and a value of .3 for ε (the ratio of the wave height to the still water depth) is chosen for the sensitivity study. Different mesh resolutions, $\mathrm{d}x = .05$ m and .1 m in the x direction and $\mathrm{d}y = .05$ m and .1 m in the y direction are used, respectively. Time steps of .001 s and .005 s are studied. The obtained results show that there are no significant differences on the achieved wave profiles. Therefore, the cell dimensions $\mathrm{d}x = .05$ m in the x direction and $\mathrm{d}y = .05$ m in the y direction are selected for this verification. This selection is based on the consideration for the requirements of the aspect ratio of the near wall mesh cells, say, the aspect ratios should be smaller than 10 in order to obtain a reasonable solution for near wall cells. Hence, we choose the finer mesh which results in more computational efforts, though a coarser mesh might be still valid. The fixed time step $\mathrm{d}t = .005$s is adopted which satisfies the requirements of the Courant Number.

Figure 2 shows the comparisons of the free surface profiles at the appropriate location of the bridge model between the numerical results and the analytical solutions for ε being .12, .18, .24, .30, .36 and .42, respectively. In such a way the values of ε employed in the following verification of the wave forces with reported laboratory measurements and in the parametric study will be within this prescribed range (i.e. from .12 to .42). These surface profiles are obtained by extracting the y coordinates of the cells where the VOF factor is .5 in the whole computational domain at a certain simulation time and then by normalising the coordinates with the corresponding water depth. The plots show that the numerical results agree very well with the analytical solutions even for a high value of ε (.30). When $\varepsilon = .36$, a phase

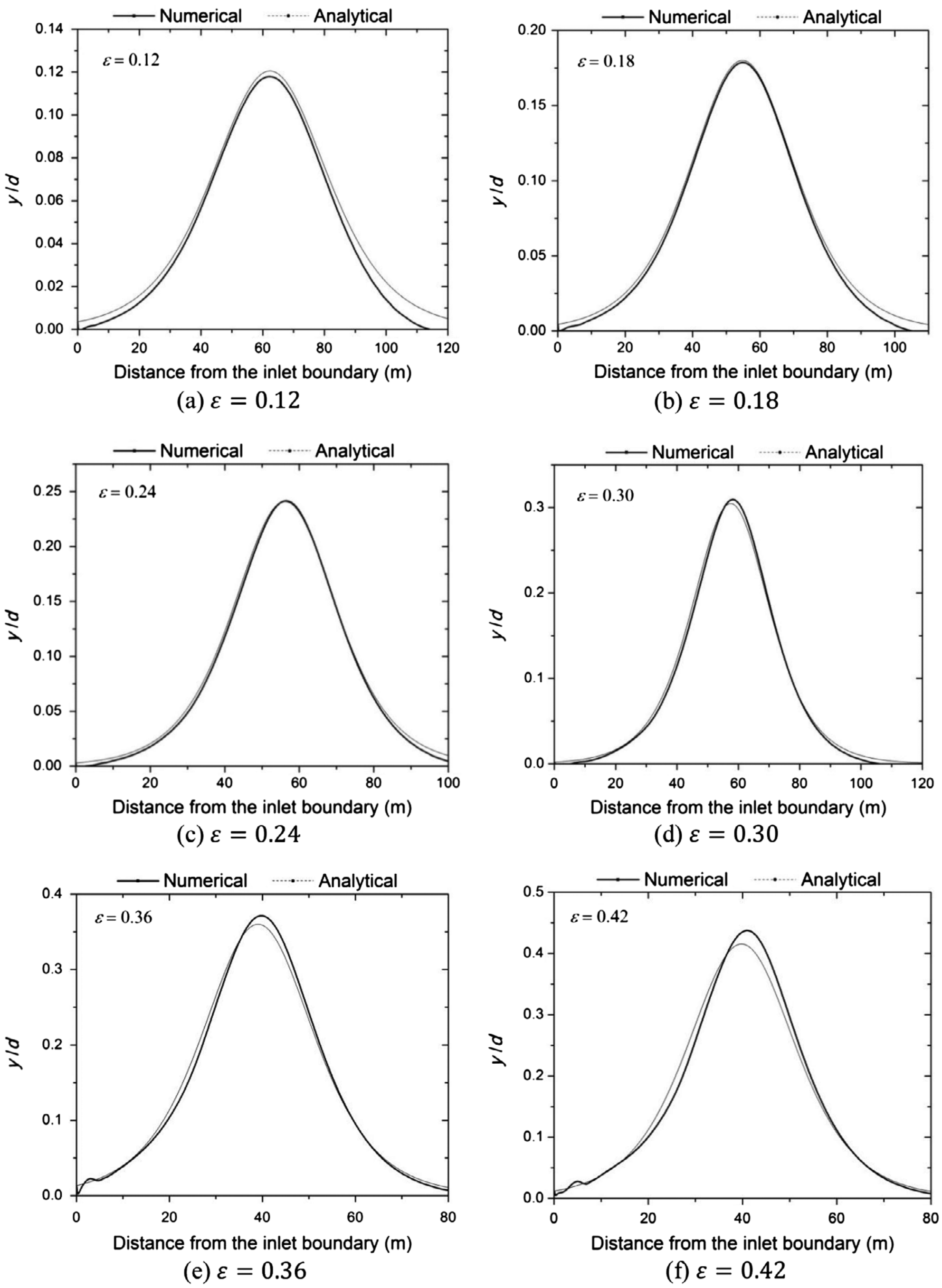

Figure 2. Free surface profiles for solitary waves near the location of the bridge model (the bridge model is placed at around 35 m in the *x* direction from the inlet boundary). *d* is the still water depth and *y* is the distance from the SWL to the water surface.

difference and a discrepancy of the wave crest between the results of the turbulent flow and the analytical method can be observed, which become larger when $\varepsilon = .42$. The critical reasons for this phenomenon are believed to include: (a) whilst the theoretical equations of the solitary waves are derived from the Navier–Stokes equations based on the in-viscid fluid assumption, there are limitations to the accuracy of the turbulent flow simulations in the current numerical model; and (b) the effects caused by the higher order terms beyond the second-order terms in the analytical solutions may be prominent when larger ratios of ε are considered. However, the results show that the difference of the wave crest of the surface profiles between the current numerical method and the analytical solutions is 5% when $\varepsilon = .42$, and much less when $\varepsilon = .36$. Thus, valid results can be expected when the wave propagates to the bridge model with the simulated surface profiles close to the prescribed ones.

Verification of the vertical wave force on a horizontal platform

In this verification, a comparison is made between the predicted wave forces using the developed wave model above and those documented in a classic laboratory experimental study conducted by French (1969), where the solitary wave-induced vertical forces

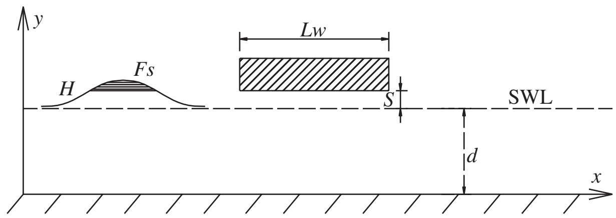

Figure 3. Experimental set-up of French (1969).

on a platform with several ratios of ε, namely, .24, .28, .32, .36 and .40 were investigated. The experimental set-up is shown in Figure 3, where F_s is the weight of water in the approaching solitary waves above the platform, marked as the shaded water area. This experimental set-up was widely employed to verify numerical results by many researchers in the literature, including Lai (1986), Huang and Xiao (2009), and Bozorgnia et al. (2010).

The parameters defined in this set-up are as follows. The computation domain is 14 m long and .7 m high; the still water depth d is .381 m; the solitary wave height H is related to ε, for example, $H = \varepsilon d = .24\, d = .0914$ m; the distance from the bottom of the platform to the still water surface, S, is .2 d = .0762 m; the length of the cross section of the horizontal platform L_W is 4 d = 1.524 m; and the height of the cross section of the platform is .2 m.

To accurately capture the near-wall features (such as the velocity field and pressure field) and hence the wave forces, much attention should be paid to the wall boundaries of the focal structure model. Based on the log-law for the 'law-of-the-wall' used for identifying the viscous layer, blending layer and the fully turbulent layer, very fine meshes are adopted near the walls of the horizontal platform. To take full advantage of the SST k-ω model, the wall-coordinate (dimensionless) $y+$ should be less than 2, where $y+$ is used to calculate the height of the first grid cell along the walls of the focal structure model in the turbulent flow. While it is very difficult to satisfy this requirement, the height of the first grid should be in the logarithmic layer and valid results can still be produced. In the literature, $y+$ is desirable to be set in a range from 11.6 to 300 in order to achieve acceptable accuracy in bridge engineering (Bredberg, 2000; Xiong, Cai, Kong, & Kong, 2014). In the current study, the range of $y+$ is from 30 to 50 in order to ensure that reliable pressure field around the near wall region can be obtained and to avoid the extensive computation.

In this verification, the grid resolutions are set as: dy = .02, .0025 and .005 m for the air zone, the near water zone and the deep water zone, respectively; dx = .005, .0025 and .02 m for the near velocity inlet zone, main computational zone and far field from the main computational zone, respectively. The time step is set as dt = .0025 s. The recorded time histories of the vertical wave forces are compared with those by French (1969) as well as some other studies (Bozorgnia et al., 2010; Huang & Xiao, 2009; Lai & Lee, 1989), as shown in Figure 4.

In Figure 4, it is observed that a larger value of ε leads to closer results to those by French (1969) in terms of the peak values in the time history curves. The possible reason is that the Iso-Surface used to separate the air phase and the water phase would be more accurate if more vertical grids are adopted in the prescribed wave height. However, in the current study the same grid mesh is employed for different ε values, which may lead to this phenomenon. Generally speaking, good agreements are obtained in the verification of the vertical wave force on a horizontal platform, which ensures a successful prediction of the wave forces in the following parametric study.

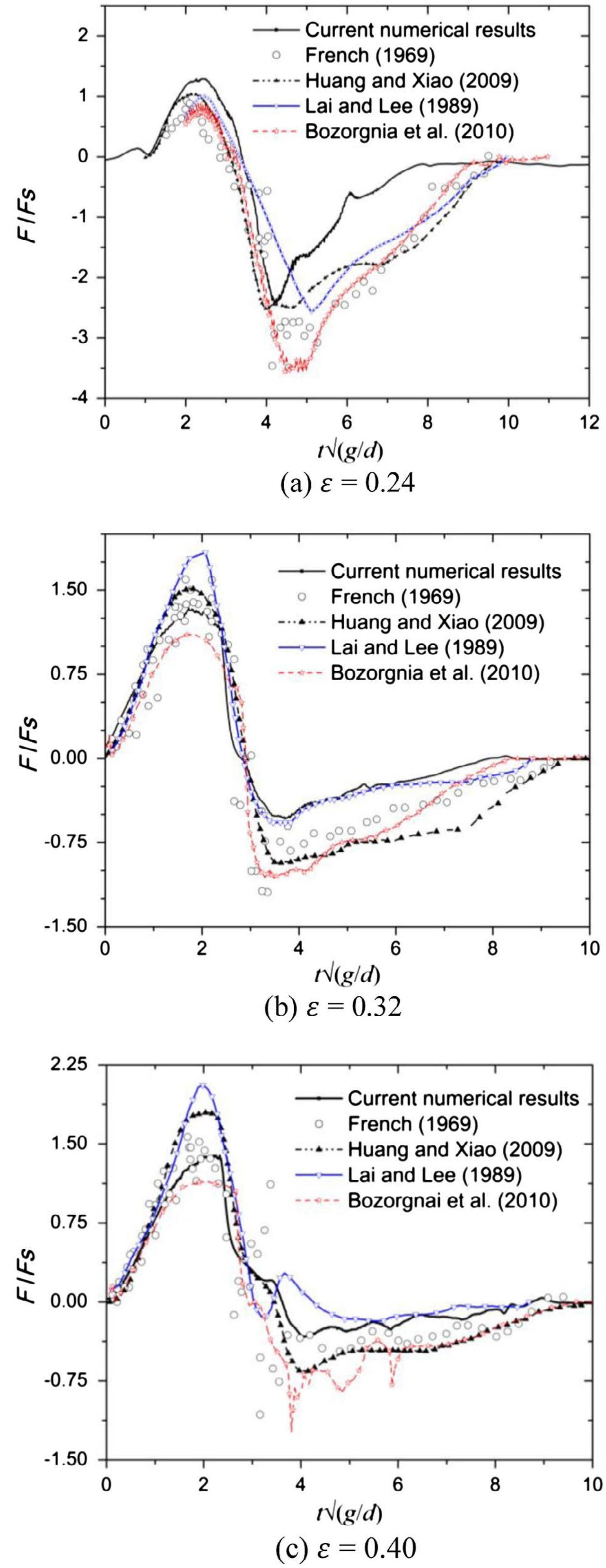

Figure 4. Comparisons of vertical wave forces between different studies.

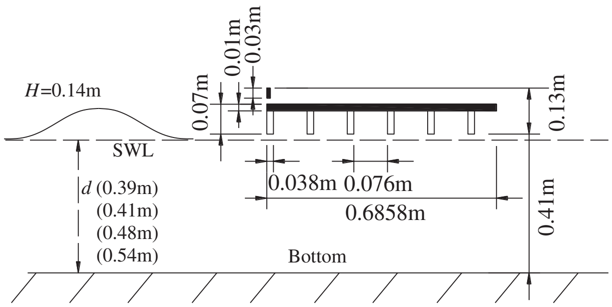

Figure 5. Schematic diagram of the bridge model for experimental set-up (McPherson, 2008).

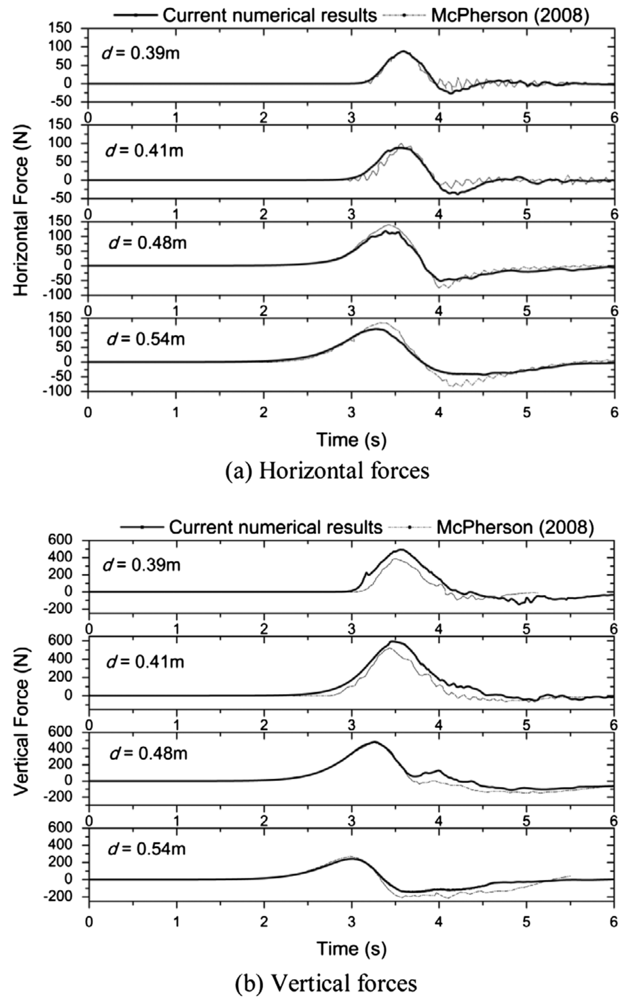

Figure 6. Verification of the wave forces on a bridge deck.

Verification of the wave forces on a bridge deck

The capability of the developed wave model to predict the wave forces is further ensured by the verification of the wave forces on a bridge deck with girders and side railings conducted by McPherson (2008) in a wave basin. The purpose of this verification is demonstrated on two distinguishable aspects: (1) the cross section of the bridge deck with girders and side railings in the laboratory study by McPherson (2008) is more complex than a horizontal platform; and (2) the verification regarding the horizontal forces needs to be confirmed. The schematic diagram of the bridge model with a 1:20 scale in the experiment set-up is shown in Figure 5, where the bottom of the bridge girders is kept at a constant height, .41 m. Four water depths, .39, .41, .48 and .54 m, are considered and one wave height, .14 m, is used. Since the perforated side railings cannot be fully realised owing to the limitation of the 2D model, a railing height of .03 m is considered above the bridge deck with a .02 m clearance in order to accommodate the experimental bridge model.

Comparisons between the results by the current method and by McPherson (2008) are shown in Figure 6. As shown in Figure 6(a), when d = .54 m, small differences between the peak horizontal forces (both the positive and negative peak values) are found. The main reason for this is that the simplified 2D railing has shortcomings when compared with the 3D perforated railings in the laboratory experiments. It is noteworthy in Figure 6(b) that differences are found between the positive peak vertical forces when d = .39 and .41 m. We attribute this to the effects of the entrapped air. In the 2D simulations, the entrapped air cannot escape in a timely manner. In summary, good and substantial agreements are witnessed in this verification, further ensuring that the current method can make successful predictions of the wave forces in the bridge deck-wave interaction problem.

Table 1. Structure elevations and corresponding coefficients.

			Momentum centre	
	S (m)	$C_s = S/H_b$	x (m)	y (m)
Case 1	.67	.5	35.225	9.07
Case 2	.30	.22	35.225	8.70
Case 3	0	0	35.225	8.40
Case 4	−.67	−.5	35.225	7.73
Case 5	−1.35	−1	35.225	7.05
Case 6	−1.65	−1.22	35.225	6.75
Case 7	−2.02	−1.5	35.225	6.38
Case 8	−2.70	−2	35.225	5.70

Parametric study

Study objects

Using the verified methodology, the characteristics of the wave forces considering different wave heights and submersion coefficients were parametrically investigated and a demonstration of the effects of the railing height on the wave forces was presented. The geometric parameters of the bridge deck model are presented earlier in Figure 1 and the computation domain is 200 m long and 13 m high, the same as that employed in the verification of the wave profiles with analytical results. Eight different bridge elevations and six different wave heights are chosen for this parametric study, see Tables 1 and 2. The as-obtained wave forces with the considered wave heights and submersion coefficients are further utilised to examine the appropriateness of some previous empirical methods.

In Table 1, the submersion coefficient C_s is defined as the ratio of S (the distance between the bottom of the girders to SWL (negative if the structure is submerged in the water)), to H_b (the height of the bridge superstructure, consisting of the deck slab and the girders). The momentum centre is the moment centre due to the vertical force and horizontal force, and it is located at

Table 2. Wave heights and related parameters for numerical simulations.

H (m)	$\varepsilon = H/d$	L_e (m)	c (m/s)	$t_0 = L_{min}/c$ (s)	Calculation time t (s)	dt (s)
3.00	.42	40.6	10.0	5	16	.002
2.60	.36	43.7	9.8	6	17	.002
2.20	.30	47.5	9.6	6	18	.002
1.74	.24	53.4	9.4	7	18	.002
1.30	.18	61.7	9.1	8	19	.002
.87	.12	75.5	8.9	9	22	.002

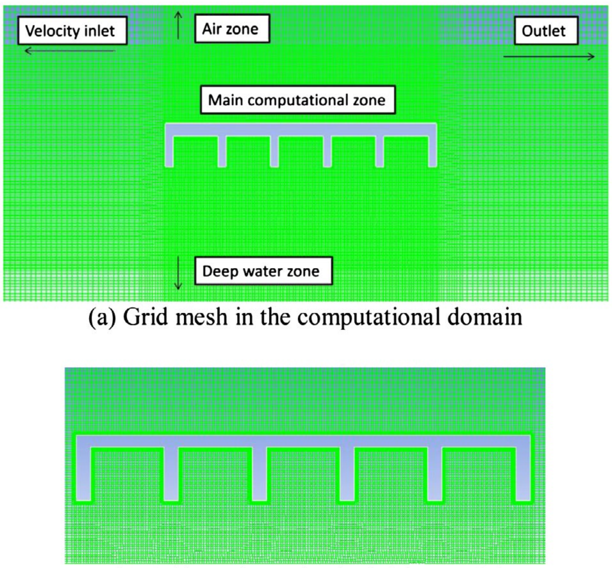

(a) Grid mesh in the computational domain

(b) Grid mesh nearby the bridge model

Figure 7. One example of the grid mesh.

the middle height of the deck for each case. The still water depth d is 7.2 m and the range of the bridge elevations (distance from the seabed to the bottom of the superstructure) represents a large variety of bridge elevations that can be normally seen in coastal areas. In Table 2, it is noticed that the higher the wave height is, the faster the wave travels and the less calculation time (from the commencement of the simulation to the time the wave crest propagates far away enough from the bridge model) needed for one simulation. The run time for one case is about 110 cpu hours, varying with the wave heights and simulation time. The time is based on 64-bit processors with a frequency of 2.6 GHz and 2 G random-access memory.

Figure 7 displays an example of the model grid mesh adopted in the computational domain. The grid resolutions are: dx = .2, .05 and .2 m for the near velocity inlet zone, main computational zone and far field from the main computaional zone (outlet), respectively; dy = .2, .05 and .1 m for the air zone, the near water zone and the deep water zone, respectively.

Time-history of wave forces

The time histories of wave forces predicted for all the eight cases when the wave height is 1.74 m are demonstrated in Figure 8. For the horizontal forces as shown in Figure 8(a), it is observed that the peak values vary with the change of the submersion depth and the positive peak horizontal force is about 1.5–2.0 times of the corresponding negative peak horizontal force for each case.

For the vertical forces in Figure 8(b), the positive peak vertical force is significantly larger than the corresponding negative peak vertical force for Cases 1–3 and the vertical force for Cases 5–8 at the initial stage (with values around 50 kN) are recognised as the buoyancy force owing to that the bridge deck is fully submerged in these cases. The positive peak horizontal and vertical forces are mainly employed to analyse the effects of the submersion coefficients on the wave forces in the next section.

Figure 9 demonstrates the snapshots of the bridge deck-wave interaction for Case 2 with the solitary wave height 1.74 m at several time points. Because the air phase is set as incompressible in the current simulations, the entrapped air is obviously captured between the girders underneath the deck. It is expected that the use of the incompressible air would not have much effects on the predicted results (Hayatdavoodi et al., 2014; Seiffert, 2014).

Effects of submersion coefficients on wave forces

The predicted positive peak wave forces with different submersion coefficients for different wave heights are shown in Figure 10, respectively. In Figure 10, it is noteworthy that the maximum horizontal forces occur at Case 6, i.e. $C_s = -1.22$, for the six wave heights studied, the same as observed in Figure 8(a). While for the vertical forces as shown in Figure 10(b) (normalised by the self-weight of the bridge deck, F_b = 95.3 kN, which is calculated based on the study by Xiao, Huang, & Chen, 2010, where the bridge span weight is 154 metric tons and the deck length is 15.85 m), the maximum positive peak vertical force appears in Case 5 ($C_s = -1.0$) for H = .87 m and in Case 3 ($C_s = 0$) for the other five wave heights. It is found that when the submersion coefficient falls in the range from −1.0 to 0, the positive peak vertical forces are relatively larger. It is also interesting to notice that the positive peak vertical forces surpass the bridge's self-weight when H = 2.20, 2.60 and 3.00 m for all the eight cases studied. For Case 3, i.e. when the bottom of the superstructure is just at the SWL, the positive peak vertical force is 1.16, 1.40, 1.93 and 2.11 times of the bridge's self-weight when H = 1.30, 1.74, 2.20, 2.60 and 3.00 m, respectively.

To resist the horizontal forces, many practical countermeasures are usually adopted in coastal bridges. The reported data pertaining to the resistant capability of the bolt systems in the study by Douglass, Chen, Olsen, Edge, and Brown (2006) is utilised here in order to obtain a perspective of the relationship between the wave loadings and the bearing capacity of the bridge deck. Douglass et al. (2006) predicted that the total resistance provided by the bolt system per span is about 890 kN (200 kips) to 1779 kN (400 kips), much larger than the predicted horizontal force from the current study, 676 kN per span (42.66 kN/m, for Case 6 with the wave height 3.00 m). In other words, the horizontal force only generated by a 3.00 m solitary wave cannot

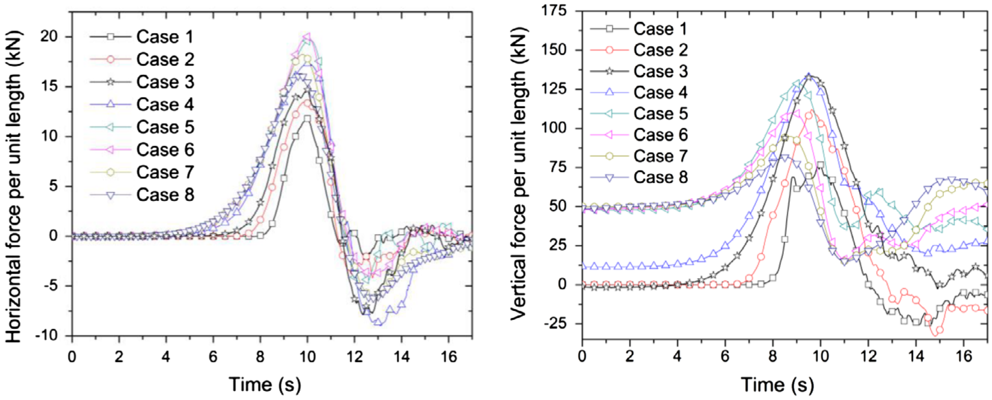

(a) H =1.74 m, Horizontal (b) H =1.74 m, Vertical

Figure 8. Demonstration of the time histories of solitary wave forces.

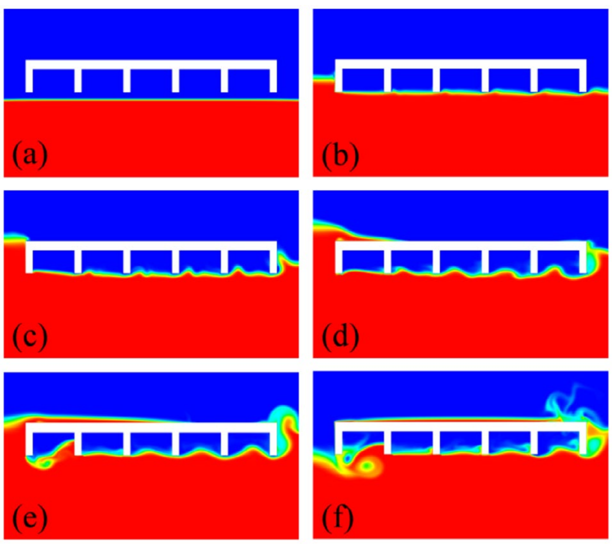

Figure 9. Snapshots of the bridge deck-wave interaction for Case 2 with the solitary wave height 1.74 m. The red colour refers to the water phase, while the blue colour refers to the air phase. (a) t = .0 s; (b) t = 8.0 s; (c) t = 9.0 s; (d) t = 10.0 s; (e) t = 11.0 s; (f) t = 12.0 s.

cause much damage to the bridge bolt system and then the superstructure. However, the positive peak vertical force for Case 6 with the corresponding wave height (H = 3.00 m) is much larger than the self-weight of the bridge deck (see Figure 10(b)), which, accompanied with the corresponding horizontal force, could easily displace or move the superstructure.

Effects of the railing height on wave forces

An additional effort is made to investigate the effects of the railing on the wave forces since only a few studies have been reported on the bridge deck models with railings (AASHTO, 2008; McPherson, 2008). In this study, the railing heights of .3 and .6 m (solid railings on both sides) are added to the original bridge model for Cases 1–3 with the wave height 2.20 m. The predicted results for these cases are listed in Table 3, where the force ratios are considered by taking the value when the railing height is 0 m as the referenced value. This table shows that the positive peak vertical forces and horizontal forces tend to increase with the increase in the railing height. However, the railing has larger effects on the horizontal forces than on the vertical forces. It is noted that more studies considering multiple variables (i.e. the height of solid railings and/or perforated railings, one side or two sides) would ensure a better understanding of the railing effects on the wave forces.

Comparisons with previous empirical methods

It is found in the literature that Douglass et al. (2006), McConnell, Allsop, and Cruickshank (2004), Cuomo, Tirindelli, and Allsop (2007), and Boon-intra (2010) established empirical formulae for predicting wave-induced forces on coastal structures (including the bridge decks) other than solitary waves and McPherson (2008) developed a method to assess the wave loadings under both the periodical waves and solitary waves. In the current study, the appropriateness of these procedures will be examined and expanded/improved, if necessary, to the cases of the solitary wave-induced forces on a typical coastal bridge deck with girders. Some other methods, such as Coastal Engineering Manual (U.S. Army Corps of Engineers, 2002) and ASCE/SEI7-05 (2006), are also found to predict wave forces on coastal structures. However, they are not utilised here in the current study with the following reasons: (a) for Coastal Engineering Manual (U.S. Army Corp of Engineers, 2002), it is indicated that physical model tests are needed to recalibrate the corresponding coefficients adopted in the prediction equations; (b) ASCE/SEI7-05 (2006) deals with wave forces on wall kind of coastal structures and they may be not suitable for assessing the wave forces on bridge decks that have relatively narrow horizontally projected areas.

McConnell et al.'s (2004) empirical method

Based on a series of experimental studies on jetties (Allsop & Cuomo, 2004; McConnell, Allsop, Cuomo, & Cruickshank, 2003; Tirindelli, Cuomo, Allsop, & McConnell, 2002), McConnell et al. (2004) provided the following empirical equations to predict wave forces on structure elements for jetty structures:

$$\frac{F_{\mathrm{vqs}(+\mathrm{or}-)}}{F_{\mathrm{v}}^{*}} = \frac{a}{\left[\frac{(\eta_{\max}-S)}{H}\right]^{b}} \tag{5a}$$

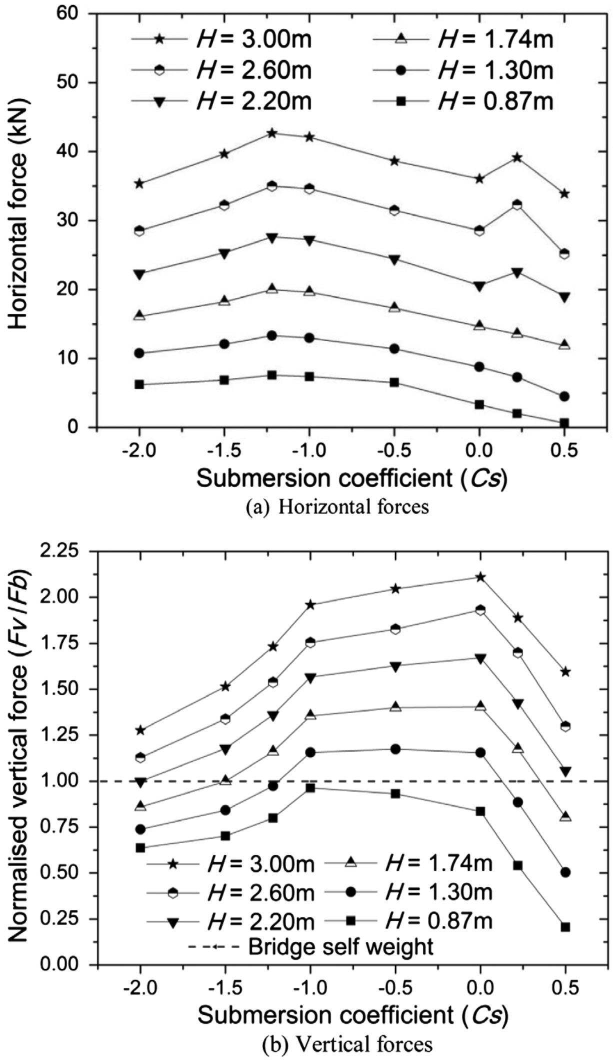

Figure 10. Variation of positive peak wave forces per unit length with submersion coefficient for different wave heights. (F_v refers to the positive peak vertical force and F_b refers to the self-weight of the bridge deck per unit length).

$$\frac{F_{\mathrm{hqs}(+\mathrm{or}-)}}{F_{\mathrm{h}}^{*}} = \frac{a}{\left[\frac{(\eta_{\max}-S)}{H}\right]^{b}} \tag{5b}$$

where F_{vqs} and F_{hqs} are quasi-static forces to be determined; F_{v}^{*} and F_{h}^{*} are the basic vertical and horizontal forces, respectively; $\eta_{\max}$ is the elevation of the wave crest; S is the clearance between the bottom of the structure to SWL; and a and b are empirical coefficients.

Douglass et al.'s (2006) empirical method

Based on the previous observations that the wave loads are linearly proportional to the difference between the wave crest and the elevation of the bottom of the structure (French, 1979; Overbeek & Klabbers, 2001; Wang, 1970), Douglass et al. (2006) developed an interim approach to predict the wave forces on typical coastal bridges using the following equations:

$$F_{\mathrm{v}} = c_{\mathrm{v-va}}\gamma(\Delta z_{\mathrm{v}})A_{\mathrm{v}} \tag{6a}$$

$$F_{\mathrm{h}} = [1 + c_{\mathrm{r}}(N-1)]c_{\mathrm{h-va}}\gamma(\Delta z_{\mathrm{h}})A_{\mathrm{h}} \tag{6b}$$

where F_{v} = vertical wave load component; F_{h} = horizontal wave load component; $c_{\mathrm{v-va}}$ and $c_{\mathrm{h-va}}$ = empirical coefficients for vertical and horizontal 'varying' loads, respectively; c_{r} = reduction coefficient for reduced horizontal load on the internal girders; N = number of girders supporting the bridge deck; A_{v} = area of the horizontal projection of the bridge deck; A_{h} = area of the vertical projection of the deck span; Δz_{v} = difference between the elevation of the wave crest and the elevation of the bottom of the bridge deck; Δz_{h} = difference between the elevation of the wave crest and the elevation of the centroid of A_{h}; and γ = unit weight of saltwater. The definition sketch for these parameters is shown in Figure 11. In the calculations employing the equations by Douglass et al.'s (2006), the parameters are defined as follows: $A_{\mathrm{v}} = 10.45\ \mathrm{m}^2$, $c_{\mathrm{v-va}} = 1$, $A_{\mathrm{h}} = 1.35\ \mathrm{m}^2$, $c_{\mathrm{h-va}} = 1$, $\gamma = 9.792\ \mathrm{kN/m}^3$, $N = 6$ and $c_{\mathrm{r}} = .4$.

Cuomo et al.'s (2007) empirical method

Similar to the guidance for evaluating wave forces on exposed jetties by McConnell et al. (2003, 2004) and Tirindelli et al. (2002), Tirindelli, Cuomo, Allsop and McConnell (2003), Tirindelli, Cuomo, Allsop, and Lamberti (2003), Cuomo et al. (2007) provides a prediction method based on separated structural elements using the filtered experimental data (Tirindelli, Cuomo, Allsop, & McConnell, 2003; Tirindelli, Cuomo, Allsop, & Lamberti, 2003) by wavelet analysis (Cuomo, Allsop, & McConnell, 2003) to account for the dynamic effects in the experimental set-up. Both the horizontal and vertical wave forces are plotted against $(\eta_{\max} - S)/d$ and non-dimensionalised by γHA, where A is the area of the element, normal to the wave forces applied. The generalised prediction equation is given as:

$$\frac{F_{\mathrm{v}} \text{ or } F_{\mathrm{h}}}{\gamma HA} = a\left(\frac{\eta_{\max} - S}{d}\right) + b \tag{7}$$

where the coefficients a and b are provided by empirical fitting.

McPherson's (2008) empirical method

Taking the Douglass et al.'s (2006) interim approach as a starting point, McPherson (2008) developed a method to examine the wave forces on bridge decks. The developed equations are given as follows:

$$\begin{aligned} F_{\mathrm{v}} &= F_{\mathrm{hydrostatic}} + F_{\mathrm{Bridge}} + F_{\mathrm{AirEntrapment}} \\ &= \gamma\delta_{Z}A_{\mathrm{v}} - F_{\mathrm{w}} + \gamma\mathrm{Vol}_{\mathrm{Bridge}} + (N-1).5\gamma\delta_{G}A_{G} \end{aligned} \tag{8a}$$

$$F_{\mathrm{h}} = F_{\mathrm{Hydrostatic\_Front}} - F_{\mathrm{Hydrostatic\_Back}} \quad \text{if } h \le h_{\mathrm{model}}, \tag{8b}$$

$$F_{\mathrm{w}} = .5\gamma\delta A_{\mathrm{v}} \quad \text{and if } h > h_{\mathrm{model}}, \tag{8c}$$

$$F_{\mathrm{w}} = .5\gamma\delta A_{\mathrm{v}} + \gamma(h - h_{\mathrm{model}})A_{\mathrm{v}} \quad \text{if } \eta_{\max} < h_{\mathrm{deck}}, \tag{8d}$$

$$F_{\mathrm{Hydrostatic\_Front}} = .5(\eta_{\max} + h - h_{\mathrm{girder}})H_{\mathrm{bridge}}L_{\mathrm{bridge}}\gamma \quad \text{and} \quad \text{if } \eta_{\max} < h_{\mathrm{deck}}, \tag{8e}$$

Table 3. Results of different railing height by current method.

	Railing height	Vertical force		Horizontal force	
		Unit: kN	Ratio	Unit: kN	Ratio
Case 1	0	97.143	1	18.67	1
	.3 m	100.4	1.034	20.274	1.086
	.6 m	109.638	1.129	22.908	1.227
Case 2	0	145.78	1	20.52	1
	.3 m	152.268	1.045	22.663	1.104
	.6 m	156.188	1.071	25.725	1.254
Case 3	0	158.003	1	19.93	1
	.3 m	160.885	1.018	23.195	1.164
	.6 m	167.151	1.058	27.134	1.361

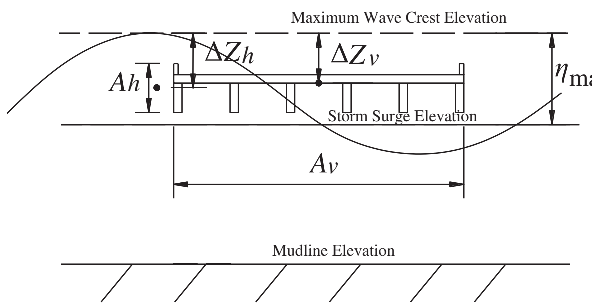

Figure 11. Definition sketch for the interim approach proposed by Douglass et al. (2006).

$$F_{\text{Hydrostatic\_Front}} = .5\left[\left(\eta_{\max} + h - h_{\text{girder}}\right) + (\eta_{\max} - h_{\text{deck}})\right] H_{\text{bridge}} L_{\text{bridge}}\gamma \quad \text{if } h < h_{\text{girder}}, \tag{8f}$$

$$F_{\text{Hydrostatic\_Back}} = 0 \quad \text{and if } h > h_{\text{girder}}, \tag{8g}$$

$$F_{\text{Hydrostatic\_Back}} = .5(h - h_{\text{girder}})^2 L_{\text{bridge}}\gamma \tag{8h}$$

where δ_Z is distance from the top of the deck to the wave crest, $\eta_{\max}$; δ_G is the height of the bridge girders; A_G is the cross-sectional area of trapped air between girders; δ is the height of wave overtopping the bridge deck; h is the height from the ground elevation to the SWL (with the same meaning as d, the still water depth); h_{model} is the distance from the ground elevation to the top of the deck; h_{girder} is the height from the ground elevation to the bottom of the bridge girders; h_{deck} is the height from the ground elevation to the bottom of the deck; H_{bridge} is the height of the bridge impacted by lateral wave forces; L_{bridge} is the length of the bridge impacted by lateral wave forces; A_v, γ, N and $\eta_{\max}$ are the same as those adopted in Douglass et al. (2006).

Boon-intra's (2010) empirical method

Based on the tsunami time-history loadings calculated from finite-element models and the studies by Douglass et al. (2006), Yeh (2007) and FEMA P646 (2008), Boon-intra (2010) suggested a method to estimate tsunami impact forces on bridge superstructures by combining the hydrostatic and hydrodynamic water pressure on deck-girder bridge sections. The suggested method was developed to be used as a preliminary guideline for design purpose due to the lack of laboratory experiments on physical bridge models. The equations are described as follows:

$$\begin{aligned} F_{\text{h}} &= F_{\text{hydrostatic}} + F_{\text{hydrodynamic}} \\ &= \left[1 + c_r(N-1)\right]\gamma(\Delta z)A_{\text{h}} + .5 \cdot C_{\text{d}}\rho(\Delta h \cdot u^2)_{\max} \end{aligned} \tag{9a}$$

$$F_{\text{v}} = F_{\text{buoyant}} + F_{\text{uplift}} = [\gamma \cdot (\Delta z) + .5 \cdot \rho u^2_{x,\max}]A_{\text{v}} \tag{9b}$$

where F_{h} consists of two parts, hydrostatic horizontal force and hydrodynamic horizontal force; F_{v} consists of two parts, buoyant force (hydrostatic vertical force) and uplift force (hydrodynamic vertical force); Δz is the distance from the bottom of girders to the instantaneous water-surface elevation (to $\eta_{\max}$ as used in the current study); $(\Delta h \cdot u^2)_{\max}$ is the maximum flux momentum; $u_{x,\max}$ is the adjusted horizontal wave velocity ($u_{x,\max} = 3.5u^*_{x,\max}$, when the bridge deck is subjected to less inundation and $u_{x,\max} = u^*_{x,\max}$ when the bridge deck is facing large inundation); $u^*_{x,\max}$ is horizontal wave velocity; C_{d} is the empirical drag coefficient ($C_{\text{d}} = 1.0$ when the bridge deck is subjected to less inundation and $C_{\text{d}} = 2.0$ when the bridge deck is facing large inundation); A_{v}, A_{h}, γ, N and c_{r} are the same as those adopted in Douglass et al. (2006). In the current study, u and $u^*_{x,\max}$ are considered as the horizontal velocities of the water particles at the SWL in order to accommodate to the solitary wave conditions (rather than breaker bores).

Comparisons and examinations of the wave forces

The predicted numerical results of the positive peak horizontal forces and vertical forces are compared with those through the empirical methods provided by McConnell et al. (2004), Douglass et al. (2006), Cuomo et al. (2007), McPherson (2008) and Boon-intra (2010) in order to identify their prediction capabilities and appropriateness of use regarding the current bridge deck model under the prescribed conditions. The comparisons for two wave heights ($H = 1.74$ and 2.20 m) are demonstrated in the sequence in Figures 12 and 13.

In Figure 12, it is observed that the predicted wave forces by Douglass et al. (2006) and Boon-intra, 2010 are significantly conservative at most times. As a matter of fact, Douglass et al.'s (2006) interim approach predicts higher wave forces when the bridge superstructure is more submerged due to the increased water level. Building on Douglass et al.'s (2006) interim approach, Boon-intra's (2010) method adds a hydrodynamic force component into the total force. As a result, the predicted horizontal forces of both methods follow the same general trend. In

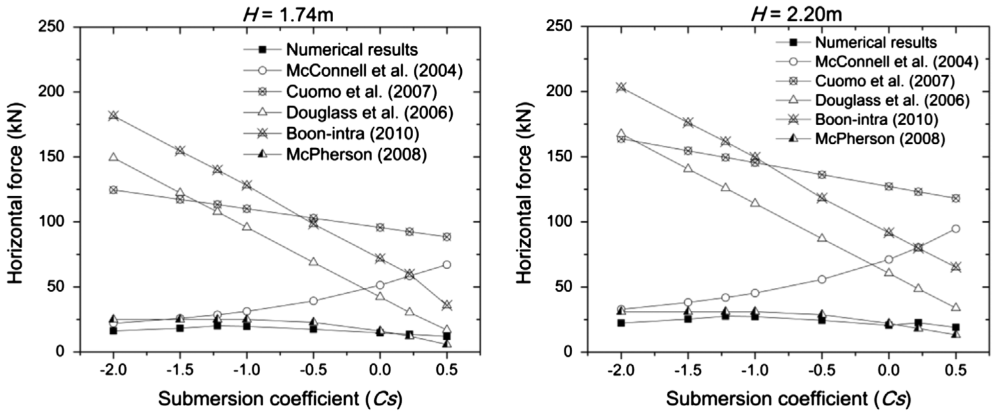

(a) $H = 1.74$ m (b) $H = 2.20$ m

Figure 12. Calculations of the horizontal forces by different methods.

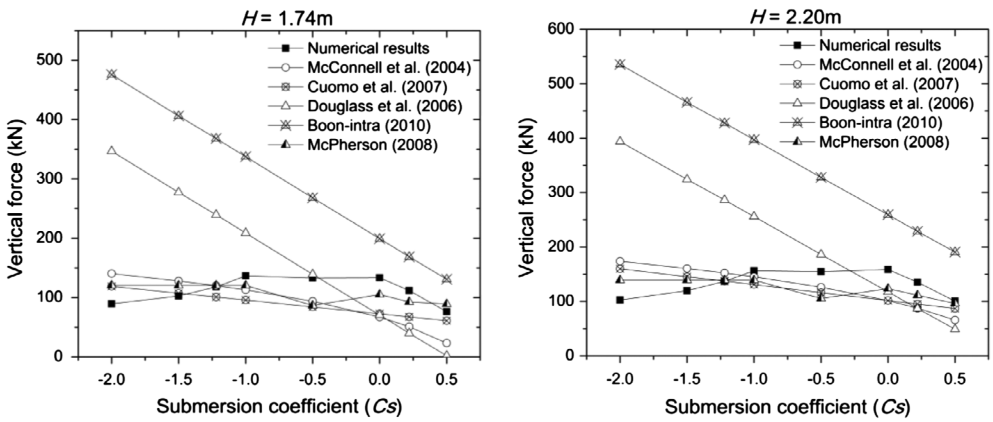

(a) $H = 1.74$ m (b) $H = 2.20$ m

Figure 13. Calculations of the vertical forces by different methods.

general, the linear increase in the horizontal wave forces with the increase in the submersion depth contradicts with the observations reported in the literature (Huang & Xiao, 2009; Jin & Meng, 2011; Xiao et al., 2010). The main reasons for this include: (1) this interim approach is not proposed for deeply submerged cases, but rather for the conditions when the bridge superstructure is located well around or suspended above the SWL; and (2) this interim approach does not distinguish the difference of wave types, e.g. Stokes waves, cnoidal wave and solitary wave. Different wave types have different horizontal and vertical velocity components, which can be reflected in the numerical simulations, but not in the empirical formulas.

The predicted forces by McConnell et al.'s (2004) and Cuomo et al.'s (2007) empirical methods, both are calibrated based on experimental measurements, also show remarkable differences with the current numerical results. Several distinct factors contributing to the differences are analysed in the comparisons of the horizontal forces: (1) the effects of the entrapped air are more prominent in the bridge deck-wave interaction in the present numerical simulations, while the air leakage and water shooting through the leakage gap was witnessed in the experiments of the jetty structure and hence influenced the developed empirical methods (Douglass et al., 2006); (2) no submerged cases were considered in the experiments; and (3) different wave types were studied. These factors results in significant differences in both the phenomena and mechanisms of the wave–structure interaction between the experimental studies for a jetty structure and the current study for a bridge deck. As such, the prediction equations originally developed for the jetty structures cannot be directly adopted to estimate solitary wave forces on bridge decks.

It is noteworthy that McPherson's (2008) method predicts much closer horizontal wave forces to those by the present numerical method as compared with other methods; however, the predicted forces are slightly larger than those by the current numerical method when the submersion coefficient is negative and smaller when positive. Apparently, McPherson's (2008) method is more appropriate for assessing the solitary wave forces on the bridge decks since the hydrostatic force on the backside is taken into account. In contrast, no water (hence the water pressure) on the trailing edge (backside) of the structures is considered for the other four methods (Boon-intra, 2010; Cuomo et al., 2007; Douglass et al., 2006; McConnell et al., 2004).

For the vertical forces as shown in Figure 13, Douglass et al.'s (2006) interim approach predicts smaller vertical forces when the submersion coefficient is positive and more conservative vertical forces when the bridge superstructure is beyond fully submerged.

Boon-intra's (2010) method predicted the same trend as that of Douglass et al.'s (2006) interim approach, but with more conservative results since the hydrodynamic force component is added into the total force. The predicted forces by McConnell et al. (2004) and Cuomo et al. (2007) almost follow the same pattern as compared with the current numerical results.

McPherson's (2008) method predicts relatively close results of the vertical forces with those by the current numerical method when the submersion coefficient is positive and around -1.0, but with some difference in the other ranges. This is maybe due to the way of treating δ_Z in the force component of $F_{\text{hydrostatic}} = \gamma\delta_Z A_v - F_w$. Strictly speaking, the water depth (and hydrostatic pressure) from the wave profile to the deck is different at different points of the deck. Simply taking δ_Z as the distance from the top of the deck to the wave crest for the whole deck may misestimate the hydrostatic force. An alternative treatment of δ_Z will be discussed later.

In summary, the methods by McConnell et al. (2004) and Cuomo et al. (2007), originally developed for the jetty structures, cannot be directly adopted to estimate solitary wave forces on bridge decks. Douglass et al.'s (2006) interim approach predicts much conservative wave forces at most times and Boon-intra's (2010) method is even more conservative since additional hydrodynamic force component is added to Douglass et al.'s (2006) interim approach. Overall, McPherson's (2008) method performs better since the water on deck force (weight of the overtopping water) and the hydrostatic force due to the existing water at the backside of the bridge superstructure are considered. Therefore, it would be more promising to further expand McPherson's (2008) method in order to make more reliable predictions for solitary wave forces on bridge decks.

Expansion of McPherson's method

The total wave forces (in the horizontal direction or in the vertical direction) can be generally divided into three components, i.e. hydrostatic force (e.g. water on deck force and buoyancy force), velocity related force (e.g. drag force and slamming force) and acceleration related force (e.g. inertia force). For the examined methods, the hydrostatic force component is usually deemed as the major part of the total forces. Therefore, these empirical methods are developed based on the analysis at the hydrostatic force level (Cuomo et al., 2007; Douglass et al., 2006; McConnell et al., 2004; McPherson, 2008). However, including the velocity related force components (based on Bernoulli's principle) that reflect the effects of the wave parameters other than the wave height, such as the wave period, wave length and wave types (AASHTO, 2008; Bea, Xu, Stear, & Ramos, 1999) may lead to more realistic results. As such, an expansion of McPherson's method is proposed by adding the velocity related components in order to provide straightforward, but advisable results of the solitary wave forces on the typical coastal bridge deck considered here.

Formulation of the expanded method

The expressions of the velocity related forces, $F_l = .5 \cdot \rho C_l A_v u^2$ and $F_D = .5 \cdot \rho C_D A_h u^2$, usually seen in the literature (for example, Bea et al., 1999), are added to the vertical and horizontal force components, respectively, in the empirical formulae suggested by McPherson's (2008), where F_l is the uplift force; F_D is the drag force; C_D and C_l are the drag and lift coefficients, respectively, and they are typically taken as 1.0 in the current study; and u is taken as the horizontal velocity of the water particle at the SWL located at the section of the wave crest and at the level of object for subaerial and submerged cases, respectively. Meanwhile, two parameters, C_w and h_{Back}, are added and one parameter, δ_Z, is adjusted. The rationality for these changes will be discussed in details later. Some of the involved parameters are shown in Figure 14 and the equations of the expanded method are expressed as follows:

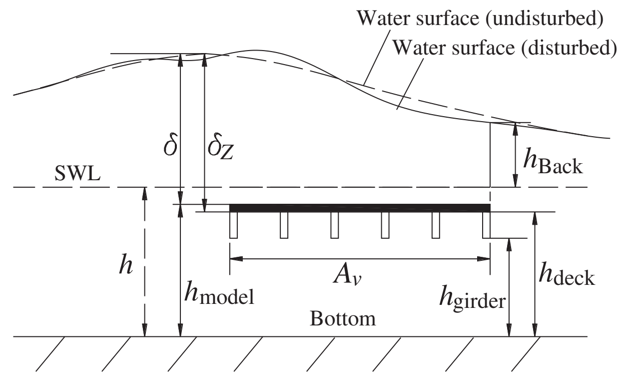

Figure 14. Schematic diagram for the parameters used in the expanded method.

$$F_v = F_{\text{Hydrostatic}} + F_{\text{Bridge}} + F_{\text{AirEntrapment}} + F_l$$
$$= \gamma\delta_Z A_v - F_w + \gamma \text{Vol}_{\text{Bridge}} + (N-1).5\gamma\delta_G A_G + .5 \cdot \rho C_l A_v u^2 \quad (10a)$$

$$F_h = F_{\text{Hydrostatic\_Front}} - F_{\text{Hydrostatic\_Back}} + F_D \quad (10b)$$

If the SWL is below the top of the deck and no overtopping water exists, i.e. $h + \eta_{\max} \le h_{\text{model}}$,

$$F_w = 0 \quad (10c)$$

if the SWL is below the top of the deck but overtopping water exists, i.e. $h \le h_{\text{model}} < h + \eta_{\max}$,

$$F_w = C_w \gamma \delta A_v \quad (10d)$$

and if the SWL is above the top of the deck, i.e. $h > h_{\text{model}}$,

$$F_w = C_w \gamma \delta A_v + \gamma(h - h_{\text{model}})A_v \quad (10e)$$

If the front girder is partially submerged, i.e. $h_{\text{girder}} < h + \eta_{\max} < h_{\text{model}}$,

$$F_{\text{Hydrostatic\_Front}} = .5(\eta_{\max} + h - h_{\text{girder}})H_{\text{bridge}}L_{\text{bridge}}\gamma \quad (10f)$$

and if the front girder is fully submerged, i.e. $h + \eta_{\max} > h_{\text{model}}$,

$$F_{\text{Hydrostatic\_Front}} = .5[\left(\eta_{\max} + h - h_{\text{girder}}\right) + (\eta_{\max} + h - h_{\text{model}})]H_{\text{bridge}}L_{\text{bridge}}\gamma \quad (10g)$$

If the back girder is above the water, i.e. $h + h_{\text{Back}} < h_{\text{girder}}$,

$$F_{\text{Hydrostatic\_Back}} = 0 \quad (10h)$$

if the back girder is partially submerged, i.e. $h_{\text{girder}} < h + h_{\text{Back}} < h_{\text{girder}} + H_b$,

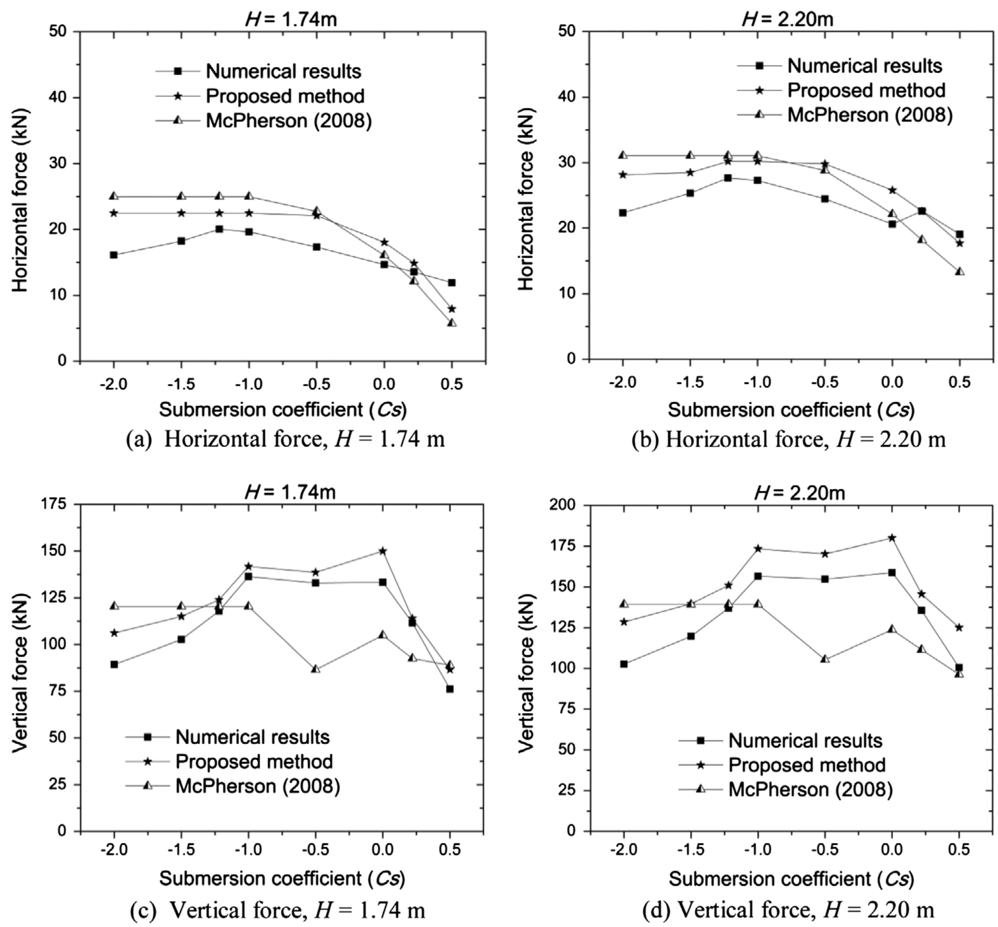

Figure 15. Comparisons of the results among current numerical results and calculations by the expanded method and by McPherson's (2008) method.

$$F_{\text{Hydrostatic\_Back}} = .5(h + h_{\text{Back}} - h_{\text{girder}})^2 L_{\text{bridge}}\gamma \qquad (10i)$$

and if the back girder is fully submerged, i.e. $h + h_{\text{Back}} > h_{\text{girder}} + H_{\text{b}}$,

$$F_{\text{Hydrostatic\_Back}} = .5(2h + 2h_{\text{Back}} - h_{\text{girder}} - h\_\text{model})H_{\text{bridge}}L_{\text{bridge}}\gamma \qquad (10j)$$

$$F_{\text{D}} = .5 \cdot \rho C_{\text{D}} A_{\text{h}} u^2 \qquad (10k)$$

where C_{w} is an empirical factor to facilitate the consideration of the water on deck. When $h \le h_{\text{model}} < h + \eta_{\text{max}}$, C_{w} is the ratio of the weight of water above the top of the deck to the corresponding value of $\gamma\delta A_{\text{v}}$.

When $h > h_{\text{model}}$, C_{w} is the ratio of the weight of water above the SWL to the weight of a rectangular column of water above the SWL, $\gamma(\delta - h + h_{\text{model}})A_{\text{v}}$. It is closely related to the shape of water on deck, say, the wave height, the width of the deck, the effective wave length and the bridge deck-wave interaction, taken as .6 when $h \le h_{\text{model}} < h + \eta_{\text{max}}$ (McPherson, 2008) to .80 when $h > h_{\text{model}}$ in the current study; δ_{Z} is the distance from the bottom of the deck to the wave crest; and h_{Back} is the possible water height above the SWL at the trailing edge of the bridge deck and it is related to the effective wave length, the wave height, the water depth, the wave speed and the geometry of the bridge superstructure. The value of h_{Back} ranges from .4 m (for smaller wave heights) to .8 m (for higher wave heights) tentatively based on the observations in the current study.

Table 4. Empirical coefficients for specified cases.

	$H = 1.74$ m		$H = 2.20$ m	
Case	C_{w}	h_{Back} (m)	C_{w}	h_{Back} (m)
Case 1	0	0	.60	0
Case 2	.60	0	.60	0
Case 3	.60	.40	.60	.50
Case 4	.60	.40	.60	.50
Case 5	.60	.40	.60	.50
Case 6	.70	.40	.70	.50
Case 7	.70	.40	.70	.50
Case 8	.70	.40	.70	.50

Improvement of the expanded method

The comparisons among the predicted results from the expanded method, the numerical results and the results calculated by McPherson's (2008) method for two wave heights, 1.74 and 2.20 m, are typically demonstrated in Figure 15. The empirical coefficients used for the specified cases are listed in Table 4. For the parameter of C_{w}, its value is 0 if there is a small tendency of the water on deck. Since a smooth shape of the water

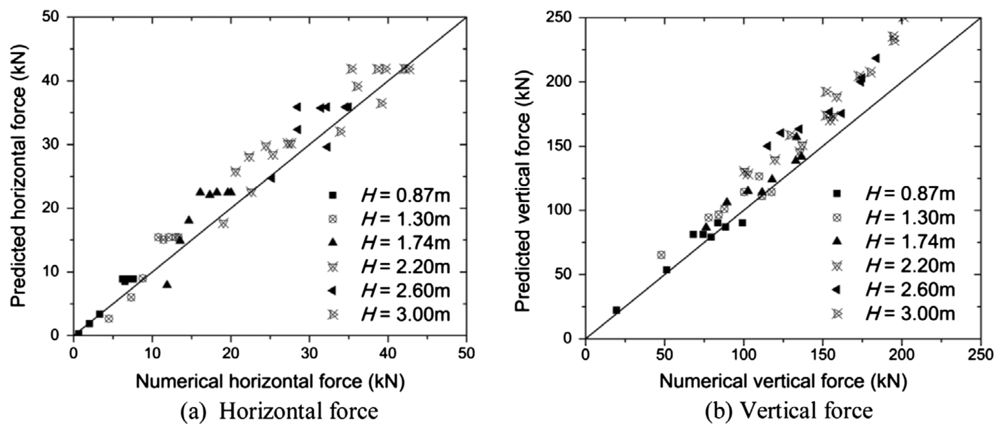

Figure 16. Comparisons of the positive peak wave forces between current numerical results and the calculated results by the expanded method.

Table 5. Comparisons of the relative error E between different methods.

	McConnell et al. (2004)	Cuomo et al. (2007)	Douglass et al. (2006)	Boon-intra (2010)	McPherson (2008)	Expanded method
F_v	.062	.052	.187	.306	.030	.024
F_h	.753	1.552	.731	1.004	.061	.032

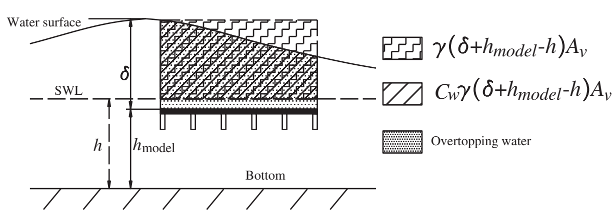

Figure 17. Schematic diagram of the estimated overtopping water.

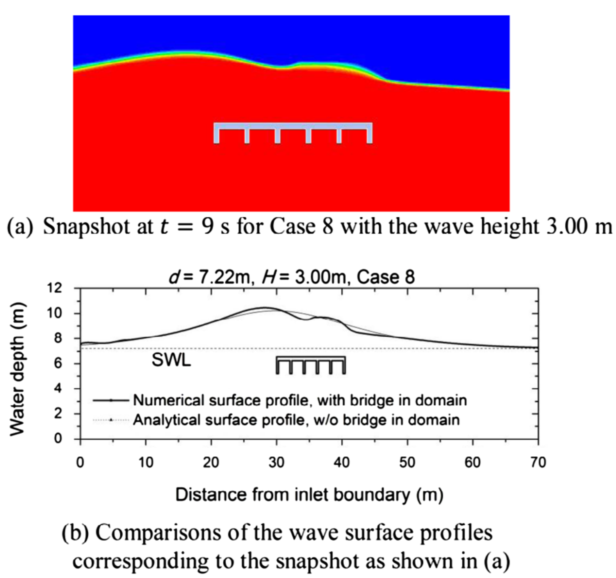

Figure 18. Demonstration of an example to estimate the overtopping water when the positive peak vertical force occurs.

on deck is observed when the bridge deck is beyond fully submerged, larger values are considered in order to obtain reasonable predictions, especially for larger wave heights. The values of .60 and .70 are taken for cases with the submersion coefficient larger than −1.0 and smaller than −1.0, respectively. Regarding the parameter of h_{Back}, it is taken as 0 when the bridge deck is subaerial (well above the SWL). Its values being .40 and .50 m are empirically chosen based on the disturbed wave profiles at the approximate time the peak horizontal forces occur when H = 1.74 and 2.20 m, respectively. These two key parameters will be further discussed later.

As observed in Figure 15, differences of the values between the predicted ones by the expanded method and the numerical results are observed. The possible reasons for the differences are believed to include: (a) the complex distribution of the pressure field on the specific projected areas may not be guaranteed to be perfectly represented by the limited parameters considered here since these parameters are empirically determined; and (b) the uncertainties of $\text{Vol}_{\text{Bridge}}$ induced by the entrapped air should be another reason for cases when the bridge deck is above the SWL. However, although the proposed expanded method predicts relatively conservative results at most times, it makes relatively better predictions than the McPherson's (2008) method.

The comparisons of the wave forces between the current numerical results and those predicted by the expanded method are plotted in Figure 16, showing a reasonable accuracy. As a result, this expanded method can serve as an alternative but convenient way to give practicing engineers a useful estimation of the wave loadings and to predict the solitary wave forces on similar kinds of deck-girder bridges. Further comparisons of this expanded method with the five examined empirical methods are made using the relative error E defined in Equation (11) and the results are shown in Table 5. The results confirm the improvement of this expanded method.

$$E = \frac{1}{n}\sqrt{\sum_{1}^{n}\left(\frac{x_i - \hat{x}_i}{x_i}\right)^2} \tag{11}$$

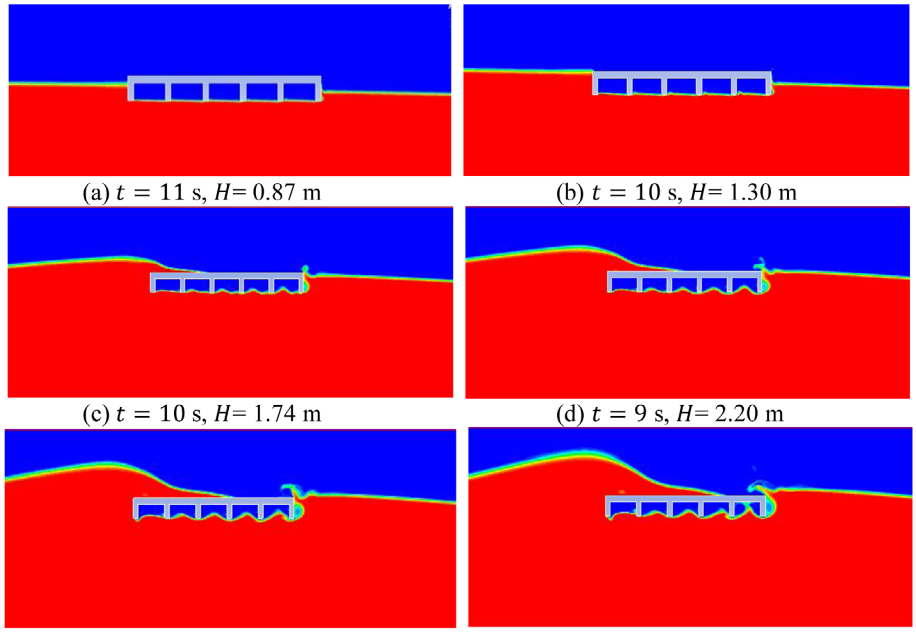

(a) $t = 11$ s, $H = 0.87$ m (b) $t = 10$ s, $H = 1.30$ m
(c) $t = 10$ s, $H = 1.74$ m (d) $t = 9$ s, $H = 2.20$ m
(e) $t = 9$ s, $H = 2.60$ m (f) $t = 9$ s, $H = 3.00$ m

Figure 19. Snapshots for empirically determining the values of h_{Back} for Case 3 with different wave heights at the approximate time when the positive peak horizontal force occurs.

where x_i and $\hat{x}_i$ are the wave forces by the current numerical method and predicted by the methods reviewed or proposed in the present study, respectively; and n is the number of tests.

Discussion of the key parameters used in the expanded method

Herein, the key parameters, C_w, h_{Back} and δ_Z, are discussed in order to give reasonable physical explanations for this proposed expanded method. In addition, the conservative performance of this method is also demonstrated in this procedure. Strictly speaking, the actual weight of water above the top of the deck and above the SWL when $h \le h_{\mathrm{model}} < h + \eta_{\mathrm{max}}$ and $h > h_{\mathrm{model}}$, respectively, should be known to calculate C_w. However, it is difficult to obtain the accurate weight of the overtopping water practically due to the disturbance of the wave profile with the presence of the bridge deck. Alternatively, an approximate estimation of C_w is considered by taking the analytical wave profiles as a base, as demonstrated in Figures 17 and 18. Figure 18 depicts an example for predicting the fraction of the water above the SWL in the overall overtopping water (in the case of $h > h_{\mathrm{model}}$). Generally speaking, C_w should be a smaller value when the effective wave length is close to or less than the width of the bridge deck. The same criteria can be used for choosing appropriate values for C_w when $h \le h_{\mathrm{model}} < h + \eta_{\mathrm{max}}$.

The parameter of h_{Back} is used to appropriately predict the hydrostatic force at the trailing edge of the bridge deck, named $F_{\mathrm{Hydrostatic\_Back}}$, at the time when the positive peak horizontal force occurs. In the proposed method, $F_{\mathrm{Hydrostatic\_Back}}$ is 0 when $h + h_{\mathrm{Back}} < h_{\mathrm{girder}}$ and this is highly expected when the back girder is above the water. However, an appropriate value of h_{Back} needs to be determined when the bridge elevation is partially submerged or fully submerged. Figure 19 demonstrates the consideration of the values of h_{Back} used in the present study, where the snapshots around the occurrence of the positive peak horizontal forces for Case 3 with different wave heights are captured. It is observed that higher wave heights are accompanied with more intense bridge deck-wave interaction. In this regard, the value of h_{Back} for the corresponding wave height needs to be empirically determined accordingly. In the current study, the value of h_{Back} is tentatively taken from .4 m (for smaller wave heights) to .8 m (for higher wave heights) based on the observation. However, this value may subject to error due to that the solitary waves may undergo significant scattering or diffraction in the bridge deck-wave interaction, especially when the bridge elevation is located around the SWL.

Additionally, the value of δ_Z in the force component of $F_{\mathrm{hydrostatic}} = \gamma\delta_Z A_v - F_w$ needs to be discussed since it is one of the reasons for making the overestimations. In the proposed method, δ_Z is defined as the distance from the bottom of the deck to the wave crest, which results in the maximum possible hydraulic pressure for the deck elements. Actually, the pressure ($\gamma\delta_Z$) on the whole projected area (A_v) can be different in different chambers as observed in Figure 20, where the gauge pressure (with respect to the operating pressure, 101,325 Pa) for three cases (Cases 1, 3 and 6) with the wave height 1.74 m at the simulation time $t = 10$ s (at the approximate time when the positive peak vertical force occurs) is plotted. Therefore, the hydrostatic force component of $F_{\mathrm{hydrostatic}}$ may be overestimated for some chambers using $\gamma\delta_Z$ for all the chambers, leading to more conservative predictions in the present study. As such, a reduction factor for $F_{\mathrm{hydrostatic}}$ would be necessary to obtain more realistic values.

In summary, the detailed discussion of the key parameters show that the proposed expanded method is able to predict the wave forces on the prescribed typical bridge deck with reasonable accuracy. The proposed method can also serve as a basis to be expanded to other cases where coastal bridges with different deck cross sections rather than the one used in the present study are considered and to scenarios where different wave parameters are involved. However, several coefficients need to be recalibrated accordingly, such as C_w, δ_Z and A_v in the equations to predict $F_{hydrostatic}$ and $F_{Hydrostatic\_Back}$, the hydrostatic force at the backside of the bridge deck.

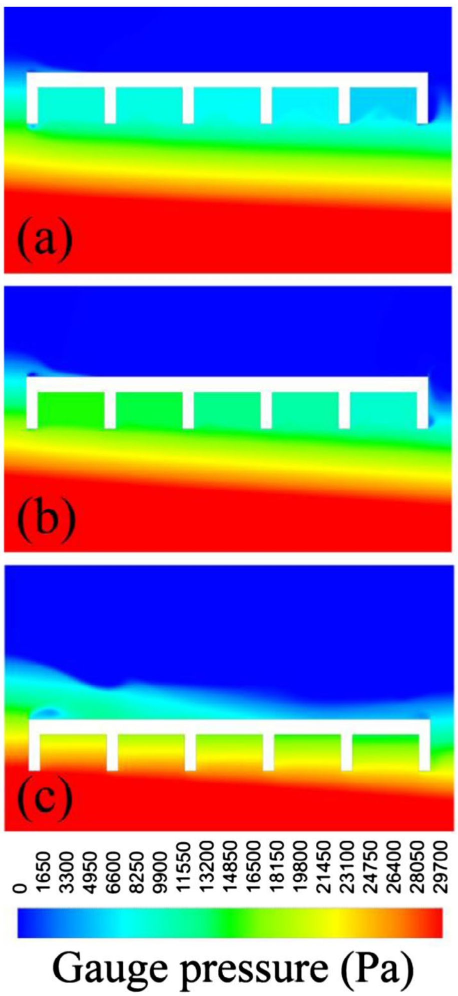

Figure 20. Gauge pressure (with respect to the operating pressure, 101, 325 Pa) for cases with the wave height 1.74 m at the simulation time t = 10 s. (a) Case 1; (b) Case 3; (c) Case 6.

Further examination of the expanded method

In order to further verify the application of the expanded method, two more different still water depths are considered, 5.4 and 9.0 m, covering a range of the water depth that coastal bridges are normally located. Four wave heights are considered here, 1.00, 1.40, 1.80 and 2.20 m. The range of the submersion coefficient is from .44 to −2.00 and there are 12 cases for each water depth, as demonstrated in Figure 21(a). The corresponding structure elevations with respect to each SWL are shown in Figure 21(b) and the vertical difference between two continuous structure elevations is .3 m. The obtained wave forces for the water depths of 5.4 and 9.0 m are plotted in Figure 22, where the results for the water depth of 7.2 m are not shown here for simplicity. The characteristics of the wave forces are similar to the observations as discussed above for the water depth of 7.2 m and hence they are not further addressed here. The details of the differences between the wave forces with the same height but different water depths were presented in the study by Xu, Cai, and Han (2015).

By employing the expanded method, the comparisons between the calculated results and the numerical results are made, as shown in Figure 23. The empirical coefficients used for cases where applicable are listed in Table 6. It should be noted that the value of h_{Back} is 0 for subaerial cases and the value of C_w is 0 if there is a small tendency of the water on deck, the same empirical rules as discussed above. The relative error E is .015 and .018 for the vertical and horizontal forces, respectively, indicating that the expanded method can predict reliable results for practical uses.

Currently, since research on the contribution of the inertial force to the total force is at the early stage for bridge deck-wave interaction problems, especially on the topic regarding solitary wave-induced loadings on bridge decks (AASHTO, 2008; Jin & Meng, 2011; McPherson, 2008), the inertia force is seldom included in these reviewed empirical methods. Though Kaplan (1992), Kaplan, Murray, and Yu (1995), and Bea et al. (1999) considered the inertial force for the horizontal cylinders and offshore

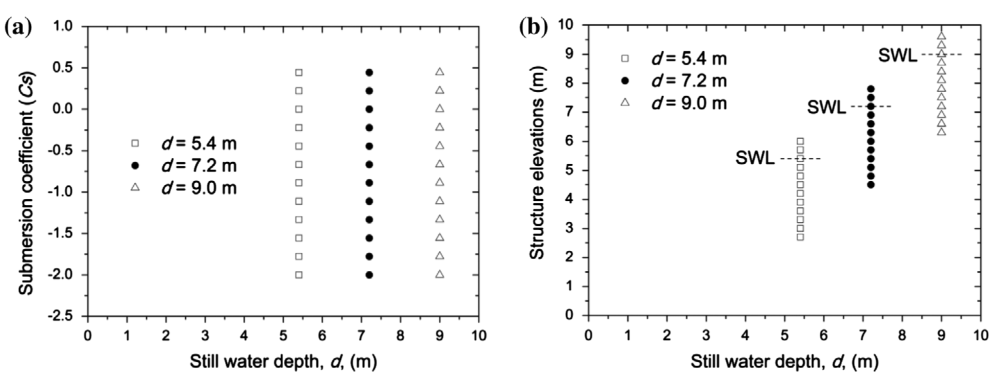

Figure 21. Further examined cases with corresponding coefficients. (a) Expressed using the submersion coefficients for each water depth; and (b) Expressed using their structure elevations for each water depth.

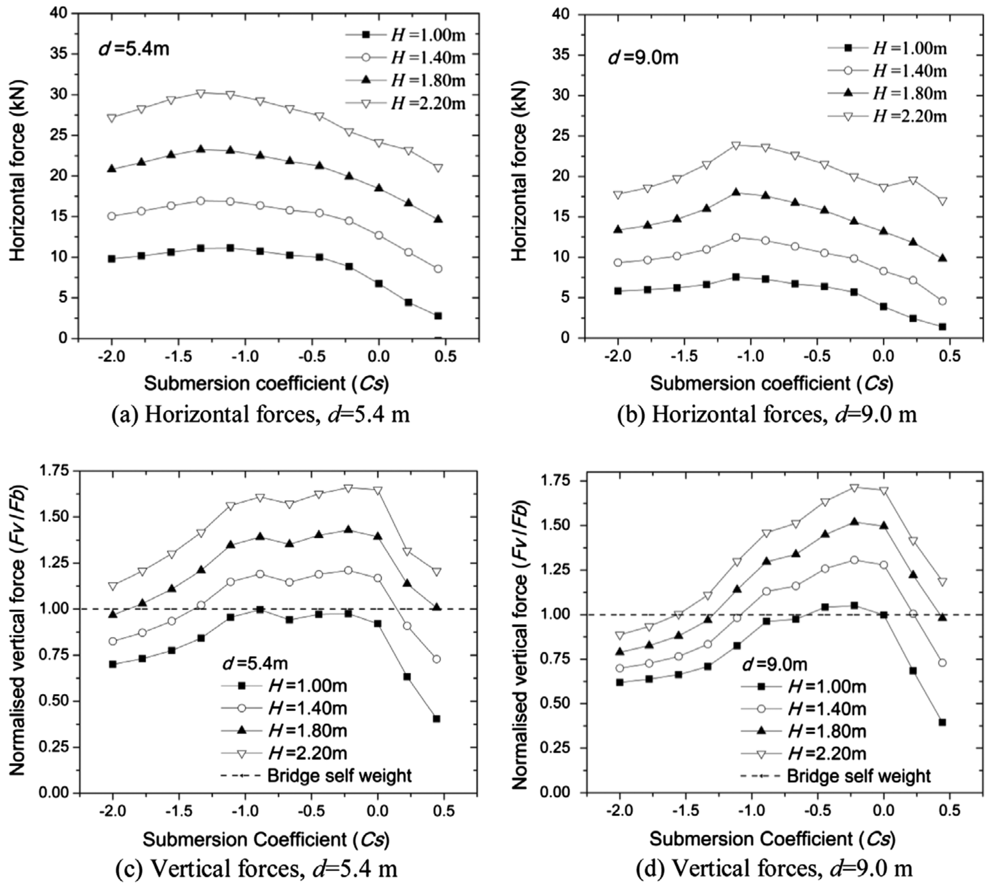

Figure 22. Wave forces on the bridge deck for the further examined cases.

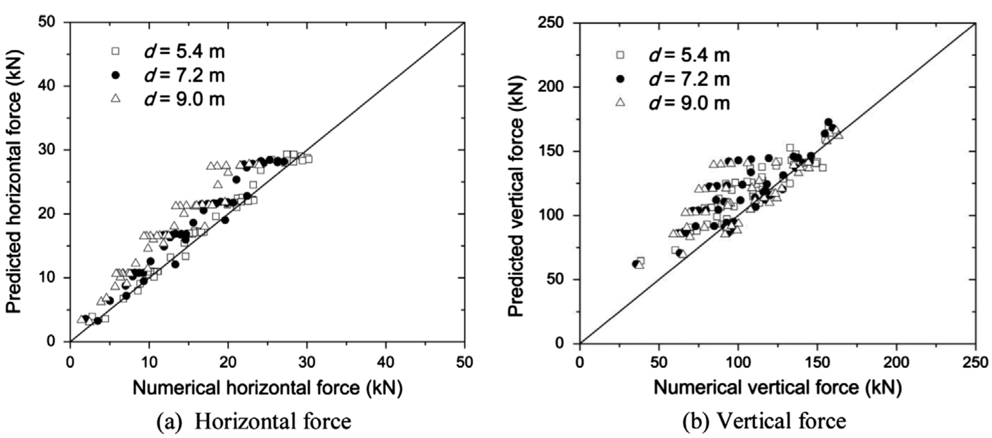

Figure 23. Comparisons between current numerical results and the calculated results by the expanded method for the further examined cases.

Table 6. Empirical coefficients for further examined cases.

	h_{Back} (m)		C_w	
Water depth (m)	$H = 1.00$ and 1.40 m	$H = 1.80$ and 2.20 m	$C_s \geq -1.0$	$C_s < -1.0$
5.4	.40	.50	.60	.70
7.2	.40	.50	.60	.70
9.0	.40	.50	.60	.70

platforms, their formulae may be not appropriate for bridge decks due to that the cross-section geometries of bridge decks are significantly different from their focal structures, such as the cylinders. However, it is feasible to more appropriately address the inertia force in the prediction equations for bridge deck-wave interactions under solitary wave conditions based on some previous studies (AASHTO, 2008; Gullett, Dickey, & Howard, 2012; Sheppard & Marin, 2009). While it is expected that the inertia force component is comparably smaller than the hydrostatic force component and the velocity related force component, it is desirable to confirm this assumption and this is left for future studies.

Conclusions

In this study, a numerical method for predicting solitary wave forces on a typical coastal bridge deck with girders is applied in order to obtain an alternative way to predict the solitary wave forces on coastal bridge decks. It is identified that this method has good capabilities to yield reliable results through the verification process with the wave profiles and with the experimental measurements. As such, it is expected that this method can be expanded to cases in which different deck cross sections rather than the typical one used in the present study are considered and to scenarios where different wave parameters are involved.

In the parametric study, the range of the bridge elevations is chosen to represent a large variety of bridge elevations in coastal areas. The range of the wave heights considered is from .87 m (ε = .12) to 3.0 m (ε = .42), which covers a considerable portion of the wave heights (ratios) studied in the literature. Numerical results show that: (1) when the submersion coefficient is from −1.0 to 0, the positive peak vertical forces are relatively larger than those at other elevations; (2) the maximum positive horizontal force occurs when the bridge superstructure is just fully submerged; and (3) while increasing the railing height results in an increase of both the horizontal force and the vertical force, the railing has larger effects on the horizontal force than the vertical force.

Based on the comparisons between the numerical results and those acquired through the empirical methods, the appropriateness of these empirical procedures in predicting the wave forces of the studied specific cases are examined. Then, an expanded formula is proposed based on McPherson's method and it is hoped that this expanded formula could provide straightforward, but advisable results for practicing engineers.

The limitations of the current study and future work are noted: (1) in the present study, 2D numerical simulations have been conducted. Three-dimensional models may provide more reliable results, but with much higher computational cost; and (2) larger wave heights that are close to the breaking wave height and the tsunami breaker bores on the coastal bridge decks need to be further studied (Lao, Lukkunaprasit, Ruangrassamee, & Ohmachi, 2010; Lau et al., 2011; Shoji, Hiraki, Fujima, & Shigihara, 2011; Thusyanthan & Martinez, 2008).

Acknowledgement

All the opinions presented here are those of the writers, not necessarily representing those of the sponsors. The writers would like to thank Professor Hong Xiao, Sichuan University, for his constructive discussions during the course of this work.

Disclosure statement

No potential conflict of interest was reported by the authors.

Funding

This work was supported by the Louisiana State University, under the Economic Development Assistantship for the first author and the NSF [grant CMMI-0927824]. The work is also partially supported by HPC@ LSU high-performance computing resources.

References

AASHTO. (2008). *Guide specifications for bridges vulnerable to coastal storms* (The AASHTO code). Washington, DC: Author.
Allsop, N. W. H., & Cuomo, G. (2004). *Wave loads on exposed jetties* (Report SR583). Oxfordshire, OX: HR Wallingford.
ASCE, SEI7-05. (2006). *Minimum design loads for buildings and other structures*. Reston, VA: ASCE Standard, American Society of Civil Engineers.
Azadbakht, M., & Yim, S. (2014). Simulation and estimation of tsunami loads on bridge superstructures. *Journal of Waterway, Port, Coastal, and Ocean Engineering*, *141*. doi:10.1061/(ASCE)WW.1943-5460.0000262,04014031
Azadbakht, M., & Yim, S. (2015). Estimation of Cascadia local tsunami loads on Pacific Northwest bridge superstructures. *Journal of Bridge Engineering*, *21*. doi:10.1061/(ASCE)BE.1943-5592.0000755,04015048
Bea, R. G., Xu, T., Stear, J., & Ramos, R. (1999). Wave forces on decks of offshore platforms. *Journal of Waterway, Port, Coastal, and Ocean Engineering*, *125*, 136–144.
Boon-intra, S. (2010). *Development of a guideline for estimating tsunami forces on bridge superstructures* (M.Sc. thesis). Oregon State University, Corvallis, OR.
Bozorgnia, M., & Lee, J. J. (2012). Computational fluid dynamic analysis of highway bridges exposed to hurricane waves. *Proceedings of 33rd Conference on Coastal Engineering*. Santander, Spain.
Bozorgnia, M., Lee, J. J., & Raichlen, F. (2010). Wave structure interaction: Role of entrapped air on wave impact and uplift forces. *Proceedings of 32nd Conference on Coastal Engineering*. Shanghai, China.
Bredberg, J. (2000). *On the wall boundary condition for turbulence models* (Internal Report 00/4). Gothenburg: Department of Thermo and Fluid Dynamics, Chalmers University of Technology.
Bricker, J. D., Kawashima, K., & Nakayama, A. (2012, March 1–4). CFD analysis of bridge deck failure due to tsunami. *Proceedings of the International Symposium on Engineering Lessons Learned from the 2011 Great East Japan Earthquake* (pp. 1398–1409). Tokyo, Japan.
Bricker, J. D., & Nakayama, A. (2014). Contribution of trapped air, deck superelevation, and nearby structures to bridge deck failure during a tsunami. *Journal of Hydraulic Engineering*, *140*. doi:10.1061/(ASCE)HY.1943-7900.0000855, 05014002
Cuomo, G., Allsop, N. W. H., & McConnell, K. (2003). Dynamic wave loads on coastal structures: Analysis of impulsive and pulsating wave loads. *Proceedings of the Coastal Structures 2003*. Portland, OR: COPRI.
Cuomo, G., Tirindelli, M., & Allsop, N. W. H. (2007). Wave-in-deck loads on exposed jetties. *Coastal Engineering*, *54*, 657–679.
Dong, Z., & Zhan, J. (2009). Numerical modeling of wave evolution and runup in shallow water. *Journal of Hydrodynamics*, *21*, 731–738.
Douglass, S. L., Chen, Q., Olsen, J. M., Edge, B. L., & Brown, D. (2006). *Wave forces on bridge decks*. Final Report for U.S. Department of Transportation, Federal Highway Administration, Office of Bridge Technology, Washington, DC.
Douglass, S. L., & Krolak, J. (2008). *Highways in the coastal environment*. (2nd ed.). Washington, DC: Federal Highway Administration. Publication No. FHWA-NHI-07-096. Print. HEC 25.
FEMA P646. (2008). *Guidelines for design of structures for vertical evacuation from tsunamis*. Washington, DC: Author.
FHWA. (2008). *Highways in the coastal environment*. Hydraulic Engineering Circular No. 25. (2nd ed.). Washington, DC: Federal Highway Administration. Publication No. FHWA-NHI-07-096.

FHWA. (2009). *Hydrodynamic forces on inundated bridge decks*. McLean, VA: U.S. Department of Transportation. Publication No. FHWA-HRT-09-028.

French, J. (1969). *Wave uplift pressures on horizontal platforms* (Report No. KH_R_19, W.M). Pasadena: Keck Laboratory of Hydraulics and Water Resources, California Institute of Technology.

French, J. (1979). Wave uplift pressures on horizontal platforms. *Proceedings of Civil Engineering in the Oceans, ASCE* (pp. 187–202). San Francisco, CA, USA.

Gullett, P. M., Dickey, M., & Howard, I. L. (2012). *Numerical modeling of bridges subjected to storm surge for mitigation of hurricane damage* (SERRI Report 70015-005). Oak Ridge, TN: Oak Ridge National Laboratory.

Hayatdavoodi, M., Seiffert, B., & Ertekin, R. C. (2014). Experiments and computations of solitary-wave forces on a coastal-bridge deck. Part II: Deck with girders. *Coastal Engineering, 88*, 210–228.

Hirt, C. W., & Nichols, B. D. (1981). Volume of fluid (VOF) method for the dynamics of free boundaries. *Journal of Computational Physics, 39*, 201–225.

Huang, W., & Xiao, H. (2009). Numerical modeling of dynamic wave force acting on Escambia bay bridge deck during hurricane Ivan. *Journal of Waterway, Port, Coastal, and Ocean Engineering, 135*, 164–175, ASCE.

Iradjpanah, K. (1983). *Wave uplift force on horizontal platform* (PhD thesis). Los Angeles: University of Southern California.

Jin, J., & Meng, B. (2011). Computation of wave loads on the superstructures of coastal highway bridges. *Ocean Engineering, 38*, 2185–2200.

Kaplan, P. (1992). Wave impact forces on offshore structures: Re-examination and new interpretations. *Proceedings of Offshore Technology Conference – 24th OTC* (pp. 79–86). Houston, TX. Paper OTC 6814.

Kaplan, P., Murray, J. J., & Yu, W. C. (1995, June). Theoretical analysis of wave impact forces on platform deck structures. *Proceedings of Offshore Mechanics and Arctic Engineering Conference, OMAE* (Vol. 1-A, pp. 189–198). Copenhagen, Demark: Offshore Technology.

Lai, C. P. (1986). *Wave interaction with structure: Hydrodynamic loadings on platforms and docks* (PhD thesis). University of Southern California, Los Angeles.

Lai, C. P., & Lee, J. J. (1989). Interaction of finite amplitude waves with platforms or docks. *Journal of Waterway, Port, Coastal, and Ocean Engineering, 115*, 19–39.

Lao, T. L., Lukkunaprasit, P., Ruangrassamee, A., & Ohmachi, T. (2010). Performance of bridges with solid and perforated parapets in resisting tsunami attacks. *Journal of Earthquake and Tsunami, 4*, 95–104.

Lau, T. L., Ohmachi, T., Inoue, S., & Lukkunaprasit, P. (2011). Experimental and numerical modeling of tsunami force on bridge decks. In: M. Mokhtari (Ed.), *Tsunami-a growing disaster* (pp. 105–130). Rijeka: InTech Publication (chapter 6).

Maruyama, K., Tanaka, Y., Kosa, K., Hosoda, A., Mizutani, N., & Nakamura, T. (2013). Evaluation of tsunami force acted on bridges by Great East Japan Earthquake. *Proceedings of 10th International Conference on Urban Earthquake Engineering* (pp. 7–16). Tokyo, Japan.

McConnell, K., Allsop, W., & Cruickshank, I. (2004). *Piers, jetties and related structures exposed to waves – Guidelines for hydraulic loading* (148 pp). London: Thomas Telford Press.

McConnell, K. J., Allsop, N. W. H., Cuomo, G., & Cruickshank, I. (2003). New guidance for wave forces on jetties in exposed locations. *Proceedings of 6th International Congress on Coastal and Port Engineering in Developing Countries, COPEDEC*. Columbo, Sri Lanka.

McPherson, R. L. (2008). *Hurricane induced wave and surge forces on bridge decks* (M.Sc. thesis). Texas A&M University, College Station.

Menter, F. R. (1994). Two-equation eddy-viscosity turbulence models for engineering applications. *AIAA Journal, 32*, 1598–1605.

Overbeek, J., & Klabbers, I. M. (2001, May 21–23). Design of jetty decks for extreme vertical loads. *Proceedings of the ASCE Ports 2001 Conference*. Washington, DC.

Sarpkaya, T., & Isaacson, M. (1981). *Mechanics of wave forces on offshore structures*. New York, NY: Van Nostrand Reinhold.

Seiffert, B. (2014). *Tsunami and storm wave impacts on coastal bridges* (Ph.D. dissertation). University of Hawaii at Manoa, Honolulu.

Seiffert, B., Ertekin, R. C., & Robertson, I. N. (2015). Wave loads on a coastal bridge deck and the role of entrapped air. *Applied Ocean Research, 53*, 91–106.

Seiffert, B., Hayatdavoodi, M., & Ertekin, R. C. (2014). Experiments and computations of solitary-wave forces on a coastal-bridge deck. Part I: Flat plate. *Coastal Engineering, 88*, 194–209.

Sheppard, D. M., & Marin, J. (2009). *Wave loading on bridge decks*. Final Report Submitted to Florida Department of Transportation, Gainesville.

Shoji, G., Hiraki, Y., Fujima, K., & Shigihara, Y. (2011). Evaluation of tsunami fluid force acting on a bridge deck subjected to breaker bores. *Procedia Engineering, 14*, 1079–1088.

Shoji, G., & Moriyama, T. (2007). Evaluation of the structural fragility of a bridge structure subjected to a tsunami wave load. *Journal of Natural Disaster Science, 29*, 73–81.

Sugimoto, T., & Unjoh, S. (2006, May). Hydraulic model tests on the bridge structures damaged by tsunami and tidal wave. *Proceedings of the 38th UJNR Joint Panel Meeting*.

Thusyanthan, I., & Martinez, E. (2008). Model study of tsunami wave loading on bridges. *Proceedings of the Eighteenth International Offshore and Polar Engineering Conference, (ISOPE)* (pp.1528–1535). Vancouver, Canada

Tirindelli, M., Cuomo, G., Allsop, N. W. H., & Lamberti, A. (2003, May 25–30). Wave-in-deck forces on jetties and related structures. *Proceedings of the Thirteenth (2003) International Offshore and Polar Engineering Conference* (pp. 562–568). Honolulu, HI.

Tirindelli, M., Cuomo, G., Allsop, N. W. H., & McConnell, K. J. (2002). Exposed jetties: Inconsistencies and gaps in design methods for wave-induced forces. *Proceedings of the 28th International Conference on Coastal Engineering (ICCE)* (pp. 1684–1696). Cardiff, UK: ASCE.

Tirindelli, M., Cuomo, G., Allsop, N. W. H., & McConnell, K. J. (2003). Physical model studies of wave-induced forces on exposed jetties: Towards new prediction formulae. *Proceedings of the Conference on Coastal Structures* (pp. 1684–1684). Portland, OR: ASCE/COPRI.

U.S. Army Corp of Engineers. (2002). *Coastal engineering manual* (Manual No. EM 1110-2-1100). Vicksburg, MS: U.S. Army Corp of Engineers, Coastal and Hydraulics Laboratory.

Wang, H. (1970). Water wave pressure on horizontal plate. *ASCE Journal of the Hydraulics Division, 96*, 1997–2017.

Xiao, H., Huang, W., & Chen, Q. (2010). Effects of submersion depth on wave uplift force acting on Biloxi Bay Bridge decks during Hurricane Katrina. *Computer & Fluids, 39*, 1390–1400.

Xiong, W., Cai, C. S., Kong, B., & Kong, X. (2014). CFD Simulations and analyses for bridge-scour development using a dynamic-mesh updating technique. *ASCE Journal of Computing in Civil Engineering, 30*. doi:10.1061/(ASCE)CP.1943-5487.0000458

Xu, G., Cai, C., & Han, Y. (2015). Investigating the characteristics of the solitary wave-induced forces on coastal twin bridge decks. *Journal of Performance of Constrtucted Facilities*. doi:10.1061/(ASCE)CF.1943-5509.0000821,04015076

Yeh, H. (2007). Design tsunami forces for onshore structure. *Journal of Disaster Research, 2*, 531–536.